Supplementary Materials

Niacin-Ligated Platinum(IV)-Ruthenium(II) Chimeric Complexes Synergistically Suppress Tumor Metastasis and Growth with Potentially Reduced Toxicity *in Vivo*

Liwei Shu,[a,b] Lulu Ren,[b] Yuchen Wang,[a,c] Tao Fang,[d] Zhijian Ye,[d] Weidong Han,[b] Chao Chen,[e,] and Hangxiang Wang[a,]**

[a] *The First Affiliated Hospital; Key Laboratory of Combined Multi-Organ Transplantation, Ministry of Public Health, School of Medicine, Zhejiang University, Hangzhou, 310003, P. R. China.*

E-mail: wanghx@zju.edu.cn

[b] *Department of Medical Oncology; Sir Run Run Shaw Hospital; School of Medicine, Zhejiang University, Hangzhou, 310016, P. R. China.*

[c] *Department of Chemical Engineering, Zhejiang, University, Hangzhou, P. R. China.*

[d] *Jinhua People's Hospital, Jinhua, Zhejiang Province, 321000, P. R. China.*

[e] *College of Life Sciences, Huzhou University, Huzhou, 313000, P. R. China.*

E-mail: chenc@zjhu.edu.cn

Experimental section

Materials

All chemicals were of reagent grade quality obtained from commercial sources and used as received. Cisplatin, [(*p*-cymene)$RuCl_2$]$_2$ (**Ru-1**), and [(Hexamethylbenzene)$RuCl_2$]$_2$ (**Ru-2**) were purchased from Tokyo Chemical Industry Co. (Shanghai, China). Hydrogen peroxide and anhydrous sodium sulfate was purchased from Tianjin Yongda Chemical Reagent Co. (Tianjin, China). Dichloromethane (DCM), dimethylformamide (DMF), dimethylsulfoxide (DMSO), tetrahydrofuran (THF), diethyl ether (Et_2O), ethyl acetate and triphosgene were purchased from J&K Chemical (Shanghai, China). AO/EB double staining kit was purchased from Beijing Solarbio Science & Technology Co., Ltd. (Beijing, China). Apoptosis detection kit was purchased from Dojindo China Co., Ltd. (Shanghai, China). Cell culture media and phosphate buffer solution (PBS) were purchased from Gino biomedical technology Co. Ltd. (Hangzhou, China).

X-ray crystallography

Light yellow crystals were harvested by Et_2O slowly diffused into a DMF solution of Pt-1. X-ray data were collected with Bruker APEX-II CCD diffractometer operating at 170(2) K using Mo Kα radiation. The crystal was kept at a steady temperature during data collection. The diffraction pattern was indexed and the unit cell was refined using **SAINT** (Bruker, V8.38A, after 2013) on 9062 reflections, 8% of the observed reflections. A multi-scan absorption correction was performed using **SADABS**-2016/2 (Bruker, 2016/2) was used for absorption correction. wR_2 (int) was 0.1005 before and 0.0733 after correction. The Ratio of minimum to maximum transmission is 0.6388. The $\lambda/2$ correction factor is not present. The absorption coefficient μ of this material is 4.825 mm^{-1} at this wavelength (λ = 0.711Å) and the minimum and maximum transmissions are 0.476 and 0.746. The structure was solved and the space group were determined by the ShelXT[1] structure solution program using dual and refined by full matrix least squares on F^2 using version 2016/6 of ShelXL[2]. All non-hydrogen atoms were refined anisotropically. Hydrogen atom positions for all of the structures were calculated and allowed to ride on their respective C atoms with C–H distances of 0.93–0.97 Å and U_{iso}(H) = –1.2–1.5U_{eq}(C).

General methods for organic synthesis

All reactions were performed in a dry atmosphere. Thin layer chromatography (TLC) was performed on silica gel 60 F_{254} pre-coated aluminium sheets (Merck) and visualized by fluorescence quenching. Flash column chromatography on silica gel (neutral, Qingdao Haiyang Chemical Co., Ltd) was used for compound purification. ^{1}H NMR (400 MHz) spectra and ^{13}C NMR (100 MHz) were recorded in DMSO-d_6 or $CDCl_3$ on a Bruker 400 spectrometer and calibrated to the residual solvent peak or tetramethylsilane (= 0 ppm). Multiplicities are abbreviated as follows: s = singlet, d = doublet, t = triplet, q = quartet, m = multiplet, dd = double doublet, dt = double triplet, br = broad. High-resolution mass spectrometry (HRMS)-ESI was recorded on AB TripleTOF 5600+ System (AB SCIEX, Framingham, USA). Infrared absorption spectrum was recorded on Nicolet iS 50 FT-IR (Thermo Fisher Scientific).

Synthesis of *c,c,t*-[$Pt(NH_3)_2Cl_2(OH)_2$]

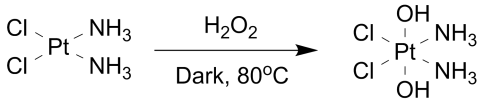

c,c,t-[$Pt(NH_3)_2Cl_2(OH)_2$] was synthesized according to the previously established protocol.[3] Briefly, a mixture of cisplatin (1.0 g, 3.3 mmol) and 30 mL hydrogen peroxide was stirred at 80℃ for 8 h in dark. After cooling at 4℃ overnight, the resulting pale-yellow precipitate was collected by filtration and washed by ethanol (5 mL × 2) and ethyl ether (5 mL × 2). Yield: 1.05 g, 95%.

HRMS: m/z calcd for $[H_8Cl_2N_2NaO_2Pt]^+$ $[M+Na]^+$ =355.9503; obsd: 355.9501.

IR (KBr) ν_{max} (cm^{-1}): 3515 (w), 3459 (br, OH), 3155 (w), 1584 (s), 1441 (s), 1379 (s), 1074 (m, Pt-OH), 860 (br), 539 [br, Pt-N(O)].

Synthesis of nicotinic anhydride

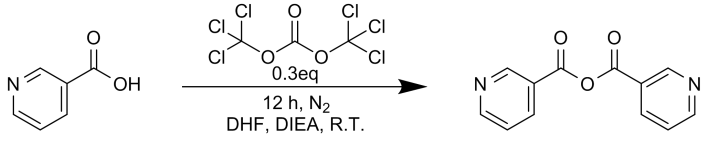

Nicotinic anhydride was synthesized according to the previously established protocol.[4] Briefly, nicotinic acid (1.2 g, 10 mmol) and triphosgene (989.1 mg, 3.33

mmol) were added to anhydrous THF at 0℃ and stirred at room temperature overnight. After removing the solvent, the residue was dissolved in ethyl acetate and washed with water and brine. The organic layer was dried over anhydrous Na_2SO_4, filtered, and evaporated under vacuum. White solid was purified through recrystallization. Yield: 1.03 g, 90%.

^{1}H NMR (400 MHz, $CDCl_3$) δ 9.37 (d, J = 2.2 Hz, 2H), 8.92 (dd, J_1 = 4.9, J_2 = 1.7 Hz, 2H), 8.43 (dt, J_1 = 8.0, J_2 = 2.0 Hz, 2H), 7.53 (dd, J_1 = 8.0, J_2 = 4.9 Hz, 2H).

^{13}C NMR (100 MHz, DMSO-d_6): δ 160.61, 160.61, 155.07, 155.07, 151.57, 151.57, 138.01, 138.01, 124.70, 124.70, 123.86, 123.86.

HRMS: m/z calcd for $[C_{12}H_9N_2O_3]^+$ $[M+H]^+$ = 229.0608; obsd: 229.0611.

IR (KBr) ν_{max} (cm^{-1}): 3082 (w), 3059 (w), 1802 (s, C=O), 1726 (s, C=O), 1053 (s, C-O-C), 1003 (s, C-O-C).

Synthesis of Pt-1

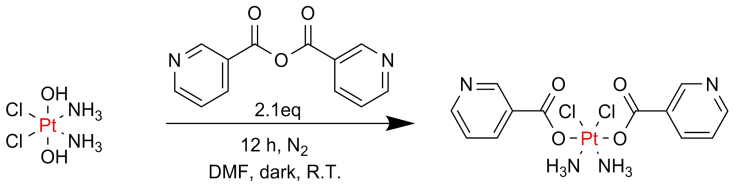

A solution of nicotinic anhydride (479.2 mg, 2.1 mmol) and *c*,*c*,*t*-$[Pt(NH_3)_2Cl_2(OH)_2]$ (334.1 mg, 1.0 mmol) in 30 mL anhydrous DMF was stirred at room temperature overnight in dark. The resulting reaction solution was concentrated to 2 mL by rotary evaporator and purified by silica gel chromatography. Yield: **Pt-1**, 244.9 mg, 45%.

^{1}H NMR (400 MHz, DMSO-d_6): δ 9.11 (s, 1H), 8.83 (d, J = 4.8 Hz, 1H), 8.36 (d, J = 8.4 Hz, 1H), 7.64 (dt, J_1 = 8.1, J_2 = 4.4 Hz, 1H), 6.36-5.55 (m, 3H).

^{13}C NMR (100 MHz, DMSO-d_6): δ 165.35, 165.35, 149.64, 149.64, 147.04, 147.04, 141.85, 141.85, 128.85, 128.85, 126.14, 126.14.

HRMS: m/z calcd for $[C_{12}H_{14}Cl_2N_4NaO_4Pt]^+$ $[M+Na]^+$ = 565.9932; obsd: 565.9933.

IR (KBr) ν_{max} (cm^{-1}): 3394 (w), 2921 (s), 2850 (m), 1647 (s).

Synthesis of PtRu-1

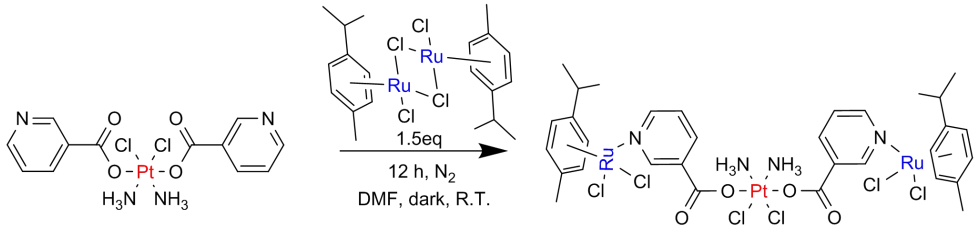

A solution of **Pt-1** (54.4 mg, 0.1 mmol) and [(*p*-cymene)$RuCl_2$]$_2$ (**Ru-1**) (92.0 mg, 0.15 mmol) in 30 mL anhydrous DMF was stirred at room temperature overnight in dark. Then, DMF was removed under vacuum. The solid residue was dissolved in DCM (3 mL) and purified by silica gel chromatography. Yield: **PtRu-1**, 63.6 mg, 55%.

^{1}H NMR (400 MHz, DMSO-d_6) δ 8.96 (dd, J_1 = 29.7, J_2 = 2.0 Hz, 2H), 8.67 (ddd, J_1 = 18.1, J_2 = 4.9, J_3 = 1.7 Hz, 2H), 8.12 (J_1 = 24.4, J_2 = 7.9, J_3 = 2.0 Hz, 2H), 7.46 (dt, J_1 = 8.0, J_2 = 4.4 Hz, 2H), 7.28 (s, 6H), 5.85-5.70 (m, 8H), 2.90-2.75 (m, 2H), 2.09 (s, 6H), 1.19 (d, J = 6.9 Hz, 12H).

^{13}C NMR (100 MHz, DMSO-d_6) δ 166.76, 166.76, 153.72, 153.72, 150.70, 150.70, 137.40, 137.40, 137.40, 137.40, 124.26, 124.26, 106.85, 106.85, 100.56, 100.56, 86.84, 86.84, 86.84, 86.84, 85.99, 85.99, 85.99, 85.99, 30.45, 30.45, 21.97, 21.97, 21.97, 21.97, 18.34, 18.34.

HRMS: m/z calcd for $[C_{32}H_{43}Cl_6N_4O_4PtRu_2]^+$ $[M+H]^+$ = 1155.9145; obsd: 1155.9142.

IR (KBr) ν_{max} (cm^{-1}): 3422 (br), 2961 (s), 1640 (s), 1470 (s), 1385 (s), 874 (w), 534.75 (br).

Synthesis of Pt-2

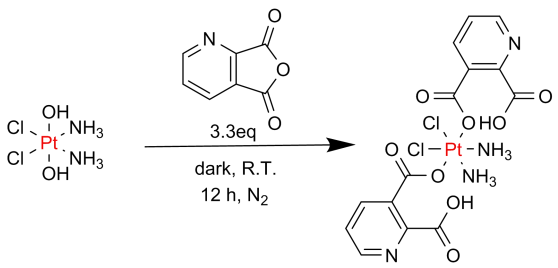

A solution of 2, 3-pyridine dicarboxylic anhydride (600 mg, 4.0 mmol) and *c,c,t*-[$Pt(NH_3)_2Cl_2(OH)_2$] (400 mg, 1.2 mmol) in 30 mL DMF was stirred at room temperature overnight in dark. Then, the yellow solution was concentrated to about 10 mL by rotary evaporator. Subsequently, 150 mL DCM was added to afford a pale-yellow precipitate. The crude product was washed with cold DCM and recrystallized in DMF/diethyl ether. Yield: **Pt-2**, 644.9 mg, 85%.

^{1}H NMR (400 MHz, DMSO-d_6) δ 13.86 (s, 1H), 8.73 (dd, J_1 = 4.8, J_2 = 1.7 Hz, 1H), 8.27 (dd, J_1 = 7.9, J_2 = 1.7 Hz, 1H), 7.58 (dd, J_1 = 7.9, J_2 = 4.8 Hz, 1H), 6.56 (s, 3H).

^{13}C NMR (100 MHz, DMSO-d_6) δ 174.51, 174.51, 167.38, 167.38, 153.46, 153.46, 151.89, 151.89, 138.58, 138.58, 125.22, 125.22, 124.28, 124.28.

HRMS: m/z calcd for $[C_{14}H_{15}Cl_2N_4O_8Pt]^+$ $[M+H]^+$ = 631.9909; obsd: 631.9907.

IR (KBr) ν_{max} (cm^{-1}): 3222 (br), 1602 (s), 1386 (s), 1324 (s), 1223 (w), 1172 (w), 1145 (w), 1092 (w).

Synthesis of PtRu-2

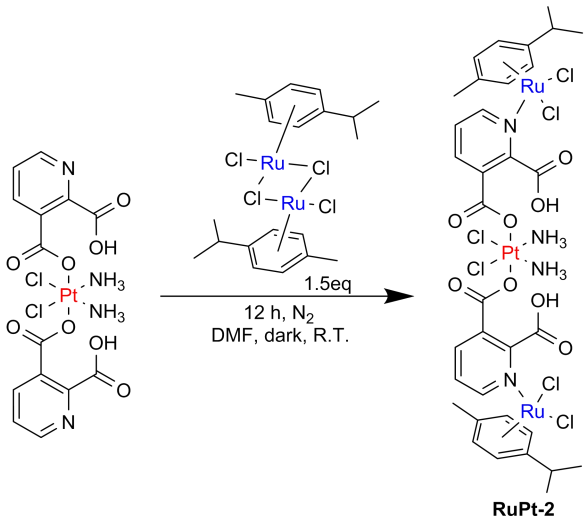

RuPt-2

A solution of **Pt-2** (63.2 mg, 0.10 mmol) and **Ru-1** (92.0 mg, 0.15 mmol) in 30 mL DMF was stirred at room temperature overnight in the dark. Then, DMF was removed under vacuum and 100 mL DCM was added to resuspend the residue. The precipitates were filtrated and discarded. The remaining supernatants were evaporated under vacuum. The crude residue was purified by silica gel chromatography to produce a claret-red powder. Yield: **PtRu-2**, 37.3 mg, 30%.

^{1}H NMR (400 MHz, DMSO-d_6) δ 13.77 (s, 1H), 9.33 (dd, J_1 = 5.5, J_2 = 1.4 Hz, 1H), 8.14 (d, J = 6.5 Hz, 1H), 7.81 (dd, J_1 = 7.8, J_2 = 5.4 Hz, 1H), 5.95 – 5.60 (m, 4H), 2.80 – 2.69 (m, 1H), 2.16 (s, 3H), 1.16 (t, J = 7.1 Hz, 6H).

^{13}C NMR (100 MHz, DMSO-d_6) δ 169.84, 169.84, 167.44, 167.44, 155.06, 155.06, 146.57, 146.57, 138.34, 138.34, 134.36, 134.36, 128.37, 128.37, 101.84, 101.84, 98.68, 98.68, 82.95, 82.95, 82.95, 82.95, 80.74, 80.74, 80.74, 80.74, 30.97, 30.97, 22.39, 22.39, 22.39, 22.39, 18.52, 18.52.

HRMS: m/z calcd for $[C_{34}H_{42}Cl_6N_4NaO_8PtRu_2]^+$ $[M+Na]^+$ = 1265.8761; obsd: 1265.8765.

IR (KBr) ν_{max} (cm^{-1}): 3422 (br), 2961 (s), 1640 (s), 1470 (s), 1385 (s), 874 (w), 544 (br), 419 (s).

Synthesis of PtRu-3

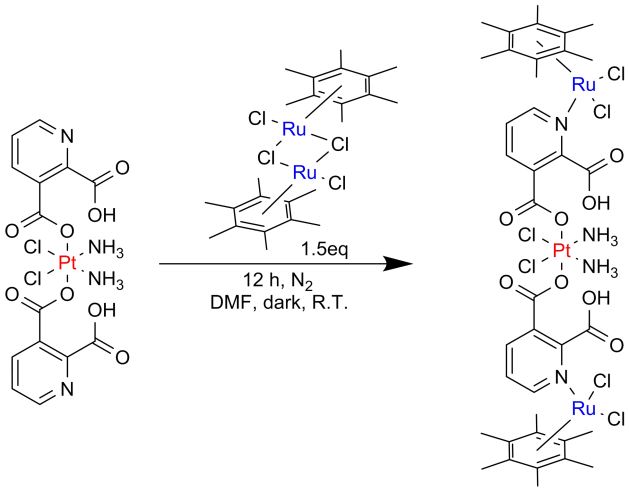

A solution of **Pt-2** (63.2 mg, 0.10 mmol) and **Ru-2** (100.3 mg, 0.15 mmol) in 30 mL DMF was stirred at room temperature overnight in dark. Then, DMF was removed under vacuum and methanol (30 mL) was added to obtain a deep-red solution. The crude residues were recovered *via* recrystallization with diethyl ether (70 mL) at 4℃. Finally, the residue was purified by silica gel chromatography to give the pure product. Yield: **PtRu-3**, 78.0 mg, 60%.

^{1}H NMR (400 MHz, DMSO-d_6) δ 14.01 (s, 1H), 8.82 (dd, J_1 = 5.5, J_2 = 1.4 Hz, 1H), 8.13 (dd, J_1 = 7.8, J_2 =1.4 Hz, 1H), 7.81 (dd, J_1 = 7.8, J_2 = 5.4 Hz, 1H), 2.06 (s, 18H).

^{13}C NMR (100 MHz, DMSO-d_6) δ 174.07, 174.07, 167.26, 167.26, 152.38, 152.38, 138.62, 138.62, 124.47, 124.47, 124.09, 124.09, 96.61, 96.61, 91.91, 91.91, 91.91, 91.91, 91.91, 91.91, 91.91, 91.91, 91.91, 91.91, 91.91, 91.91, 91.91, 91.91, 15.77, 15.77, 15.77, 15.77, 15.77, 15.77, 15.77, 15.77, 15.77, 15.77, 15.77, 15.77, 15.77, 15.77.

HRMS: m/z calcd for $[C_{38}H_{50}Cl_6N_4NaO_8PtRu_2]^+$ $[M+Na]^+$ = 1321.9387; obsd: 1321.9389.

IR (KBr) ν_{max} (cm^{-1}): 3447 (br), 1632 (s), 1386 (s), 555 (br).

Synthesis of PtRu-4

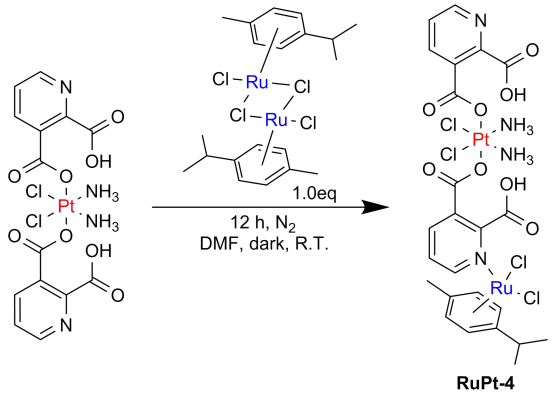

A solution of **Pt-2** (63.2 mg, 0.10 mmol) and **Ru-1** (61.2 mg, 0.10 mmol) in 30 mL DMF was stirred at room temperature overnight in the dark. Then, the reaction mixture was concentrated to about 5 mL under vacuum, and 50 mL of DCM was added to give the reddish-brown precipitates. The precipitate was collected and washed by DCM. Finally, the residue was purified by recrystallization to give the pure product. Yield: **PtRu-4**, 18.8 mg, 20%.

^{1}H NMR (400 MHz, DMSO-d_6) δ 13.87 (s, 2H), 8.73 (d, J = 4.9 Hz, 2H), 8.27 (d, J = 8.1 Hz, 2H), 7.59 (dd, J_1 = 8.1, J_2 = 4.7 Hz, 2H), 6.53 (s, 6H), 5.92-5.58 (m, 4H), 2.90 – 2.78 (m, 1H), 2.09 (s, 3H), 1.20 (d, J = 6.9 Hz, 6H).

^{13}C NMR (100 MHz, DMSO-d_6) δ 166.77, 166.77, 153.77, 153.77, 150.70, 150.70, 137.43, 137.43, 127.10, 127.10, 124.30, 124.30, 124.30, 124.30, 106.84, 100.56, 86.84, 86.84, 85.99, 85.99, 30.45, 21.98, 21.98, 18.35.

HRMS: m/z calcd for $[C_{24}H_{28}Cl_4N_4NaO_8PtRu]^+$ $[M+Na]^+$ = 959.9245; obsd: 959.9242.

IR (KBr) ν_{max} (cm^{-1}): 3439 (br), 1630 (s), 1389 (m), 1115 (w), 880 (w), 545 (br).

Reduction of PtRu-1 in the presence of sodium ascorbate

The solution of **PtRu-1** (2 mg) in DMSO-*d6*/D_2O (5:1, v/v) was added with sodium ascorbate (1.2 mg, 3.5 eq). The sample was incubated at room temperature and then was subjected to ^1H NMR measurements at the predetermined time points (i.e., 2, 5, 10, 15, 30, 60, and 120 min, and 14 h).

Cell lines and culture

Human cancer cell lines A549 (lung cancer), A2780 (ovarian cancer), SGC7901 (gastric cancer), LoVo (colon cancer) cells and human umbilical vein endothelial cells (HUVEC) were purchased from Cell Bank of the Chinese Academy of Sciences (Shanghai, China). Cancer cells were cultured in RPMI 1640 medium at 37°C in a 5% CO_2 atmosphere and HUVEC was cultured in DMEM medium. The cell culture media were supplemented with fetal bovine serum (FBS), penicillin (100 units/mL), and streptomycin (100 μg/mL).

Cytotoxicity test

The cytotoxicity of compounds against different cell lines was determined by 3-[4,5-dimethylthiazol-2-yl]-3,5-diphenyl tetrazolium bromide (MTT) assay. Cells were seeded in 96-well plates (3000 cells per well) and incubated at 37°C for 24 h. Then, the cell culture media (100 μL) containing different concentrations of the compounds were added to each well and incubated for another 72 h. At the end of incubation, 20 μL of MTT solution (5 mg/mL) was added to each well. After 4 h, the purple MTT-formazan crystals were dissolved by 200 μL DMSO and the absorbance of each individual well was determined by a microplate reader (Multiskan FC, Thermo Scientific) at the wavelength of 490 nm. Cell viability was calculated according to the following equation:

Cell viability (%) = absorbance of each well / absorbance of control well × 100%.

AO/EB double staining assay

A2780 cells were seeded in 48-well plates at a density of 1.5×10^4 cells per well and incubated at 37°C overnight. Then, the cells were treated by serial dilutions of the compounds for another 48 h. After that, all media were discarded and 200 μL AO/EB solution was added to each well. After 30 min incubation, the cells were washed with PBS and photographed under fluorescence microscopy. The cell numbers were counted from at least three fields. The apoptosis rate was calculated as follows:

Late apoptosis and necrosis rate (%) = number of cells emitting orange fluorescence / number of cells emitting green fluorescence × 100%.

Wound healing assay

Cell migration was determined by wound healing assay (migration assay). Briefly, cells (i.e., HUVEC and A2780) were seeded in 6-well plates at a density of 2×10^5 cells per well and incubated at 37°C for 24 h. After that, the wounds were scratched by 200-μL pipette tips and the suspended cells were removed by PBS. Another 500 μL of medium without FBS was added with serial dilutions of the compounds for another 48-h incubation. Migration rate was used to estimate the migration ability of cancer cells, which could be calculated as follows:

Migration rate (%) = the reduced wound width in each group at each time / the average width of initial wound in all groups × 100%.

Invasion assay

In brief, matrigel matrix (BD Biosciences, 354234) was diluted with medium (no FBS) at a ratio of 1:20. Each hanging cell culture insert (Millicell 24-well inserts, USA) was coated with 50 μL of diluted matrigel and allowed to complete gelation for 2-3 h at 37°C. Then, 200 μL of medium (2% FBS) containing 4×10^4 HUVEC cells and different concentrations of the compounds was added into the upper chamber and 700 μL of medium (20% FBS) was added into the lower chamber. All media were removed after 24 h incubation, and methanol was used to fix the cells for 30 min. Cells in the upper chamber were removed by a swab. The invading cells were stained with 0.1% crystal violet and counted from at least three fields.

Capillary tube formation assay of HUVECs

33 μL of matrigel matrix (BD Biosciences, 354234) was added to each well in 96-well plates. After gelation, the solutions containing 2×10^4 HUVEC cells and the compounds were added and incubated for 12 h. The formation of capillary-like structures on matrigel was photographed at 4 h, 8 h, and 12 h. Capillary tube length and numbers of branch points were quantified at least in three fields.

Cell cycle arrest

Flow cytometry was used to determine the proportion of cells at each phase of cell cycle. After 24 h incubation in 6-well plates, A2780 cells were incubated with the compounds for another 48 h. At the end of the incubation period, cells were collected and centrifuged. 75% ethanol was used to fix cells at 4℃ overnight. The cells were washed twice with PBS and stained with PI before analyzing the cell cycle distribution with a BD FACSCanto™ II flow cytometer.

Apoptosis

The apoptosis rate of cells upon treatment with different compounds was detected using the fluorescein isothiocyanate (FITC) Annexin V Apoptosis Detection Kit (Multi Sciences, China) by flow cytometry. A2780 cells treated with different compounds for 48 h were collected and centrifuged. A portion of untreated cells were treated with 30 sec thermal shock as positive control. All groups were stained with FITC Annexin V (5 μL) and PI (5 μL) for 15 min before submitted to FACSCalibur™ system.

Animal studies

Mice (5-6 weeks old) for animal studies were purchased from Shanghai Experimental Animal Centre, Chinese Academy of Science. All animal experiments were performed in compliance with the guidelines of the Zhejiang University Committee for Animal Use and Care. The studies involving animals were approved by The Animal Care and Use Committee of Zhejiang University. They were housed under aseptic conditions and given an autoclaved rodent diet and sterile water.

***In vivo* toxicity**

Healthy ICR mice (5-6 weeks old) were randomized into 8 groups (n = 6, females) and intraperitoneally injected with **PtRu-1** solution (200 μL) and cisplatin solution

(Hospira Australia Pty Ltd) in different doses every day for 5 times. Saline was injected as control. The changes of mice weight were monitored for 2 weeks. Mice in the same group were sacrificed once any death occurred. Three mice in each group were sacrificed by CO_2 inhalation after the last administration for histopathological analysis. Major organs (e.g., kidney, liver, heart, spleen, intestine, and stomach) were collected and fixed in 4% formaldehyde. After embedded in paraffin, tissues were sectioned into 5-μm-thick slices and stained with hematoxylin and eosin (H&E, Sigma). Tissue sections were digitized employing a whole slide scanner (NanoZoomer Digital Pathology System, Hamamatsu) and visualized in corresponding software.

Antitumor activity

A2780 (Human ovarian cancer) cells were harvested and suspended in PBS at 4°C to a final concentration of 5×10^7 cells/mL. Balb/c mice were randomized into 6 groups (n = 8) and each mouse was injected intraperitoneally with 200 μL of cell suspension. From the day 2, mice were intraperitoneally injected with 200 μL of **PtRu-1** solution (at a dose of 0.75, 1.5 and 3 mg/kg, cisplatin equivalent), cisplatin (at 0.75 mg/kg), and **Ru-3** at 6 mg/kg every day for 5 times. The control group was treated with 200 μL of saline. The tumor volume and body weight were monitored and recorded. Mice were sacrificed by CO_2 inhalation after 33 days. All tumors in abdominal cavity and ovaries were collected. Metastasized tumors in the liver and spleen were counted and recorded. No metastases were found in other organs.

Statistical analysis

All quantitative data are presented as means ± SD. The significance of the compared measurements was evaluated using two-tailed unpaired Student's *t*-test. A *p*-value of less than 0.05 was considered significant, while a *p*-value of less than 0.01 was considered highly significant.

Supplementary Figures

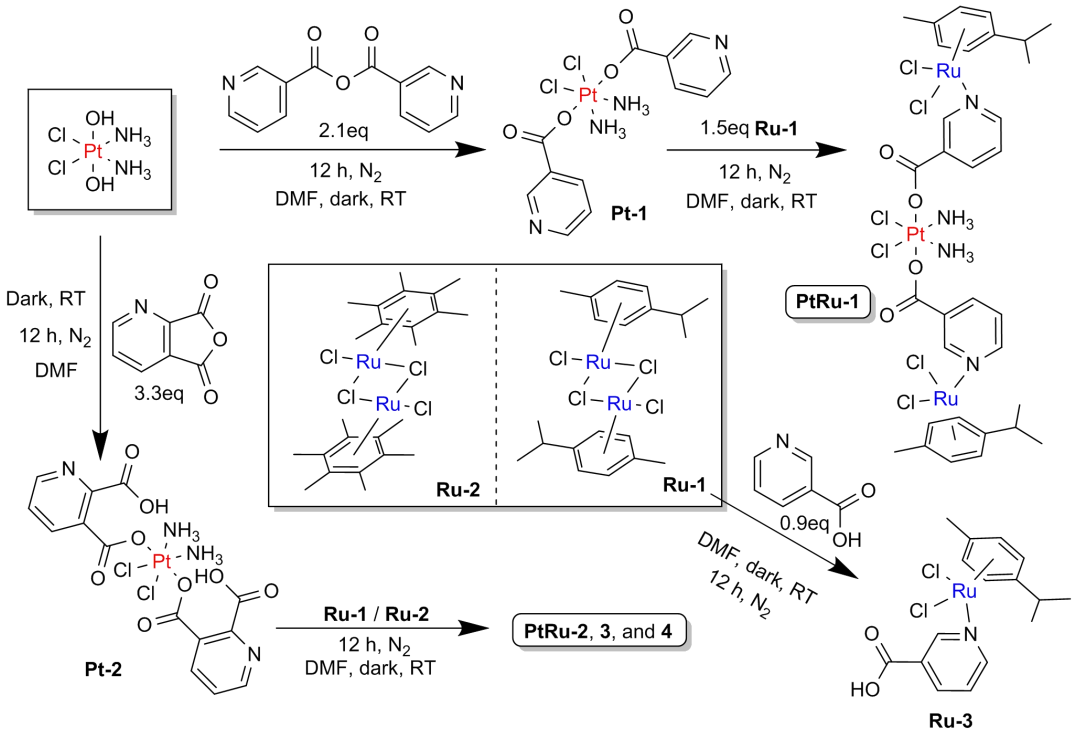

Scheme S1. Synthetic scheme.

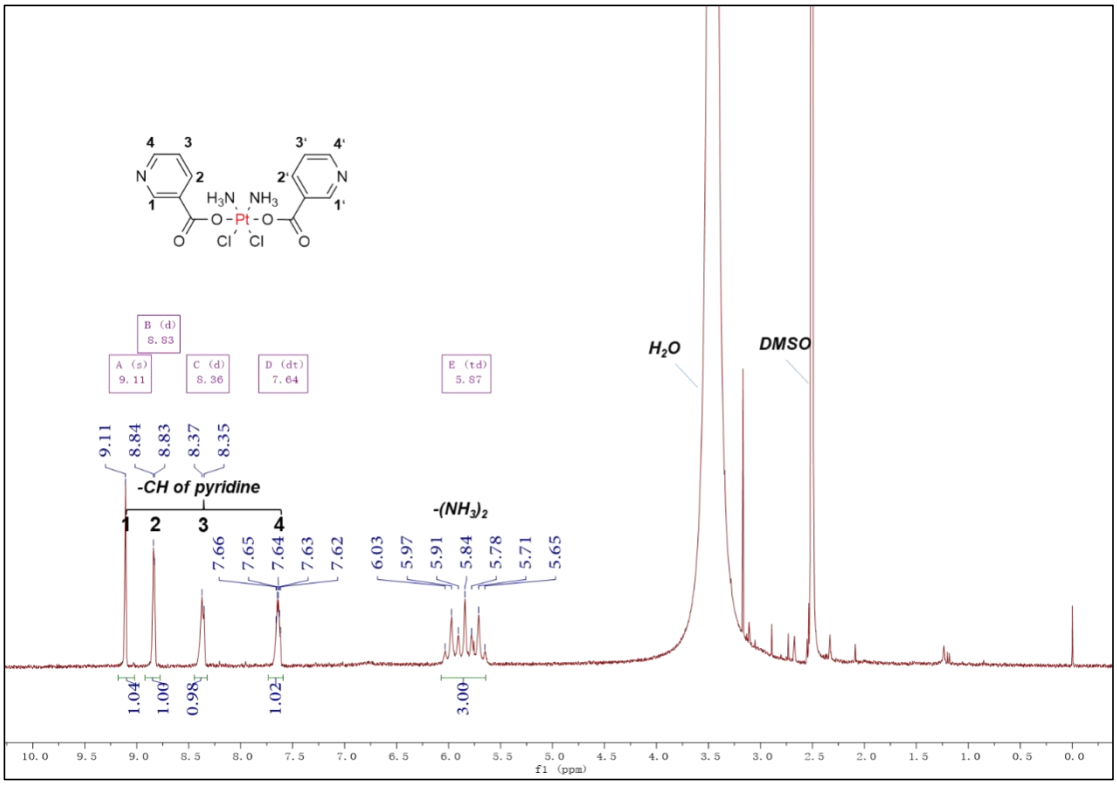

Figure S1. ^{1}H NMR spectrum of **Pt-1** measured in DMSO-d_6.

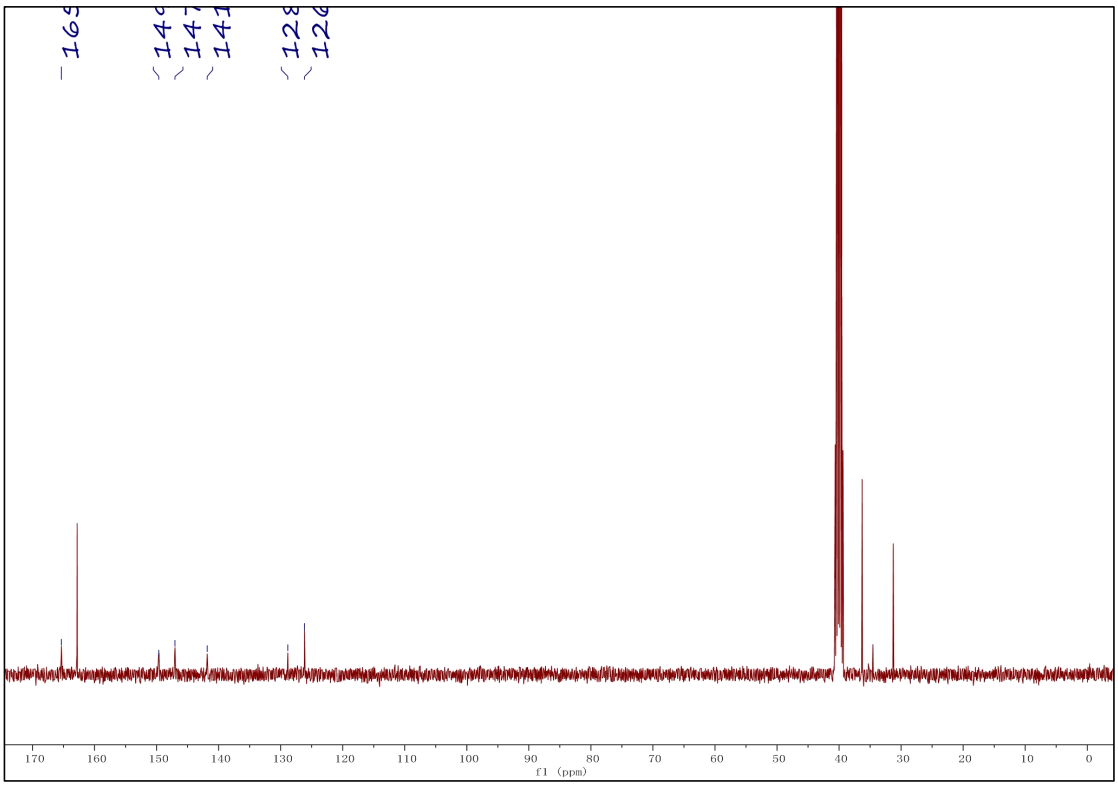

Figure S2. ^{13}C NMR spectrum of **Pt-1** measured in DMSO-d_6.

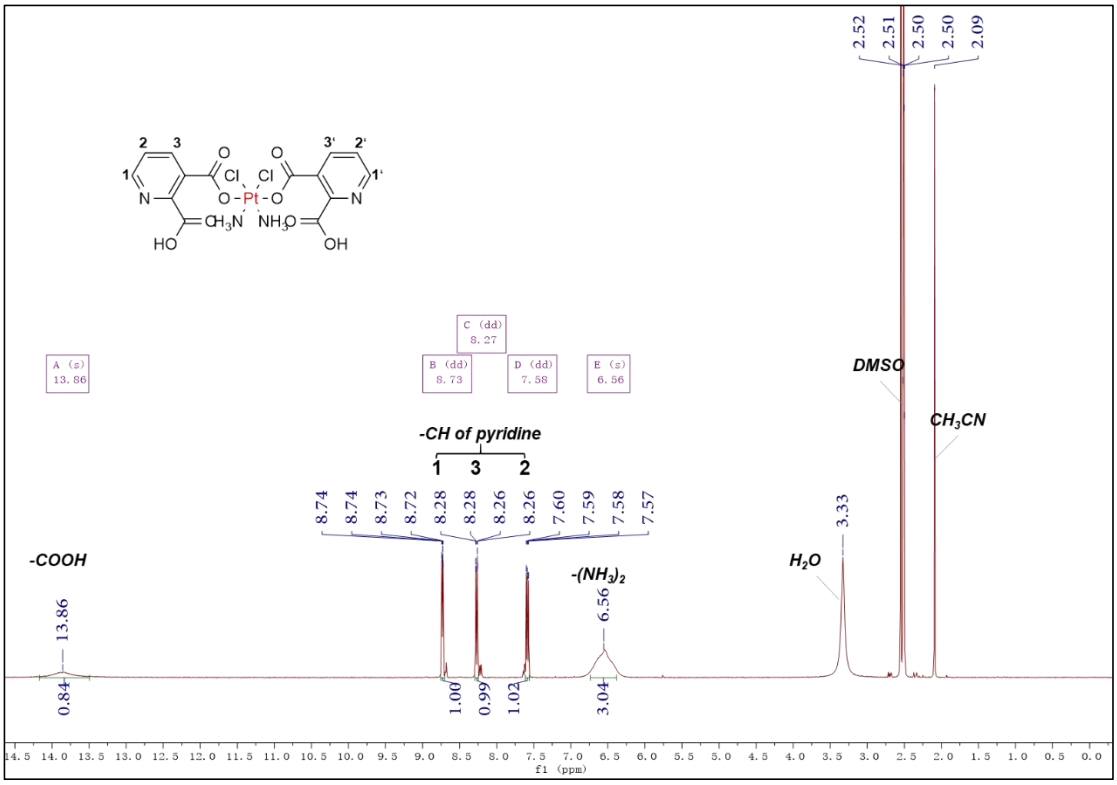

Figure S3. ^{1}H NMR spectrum of **Pt-2** measured in DMSO-d_6.

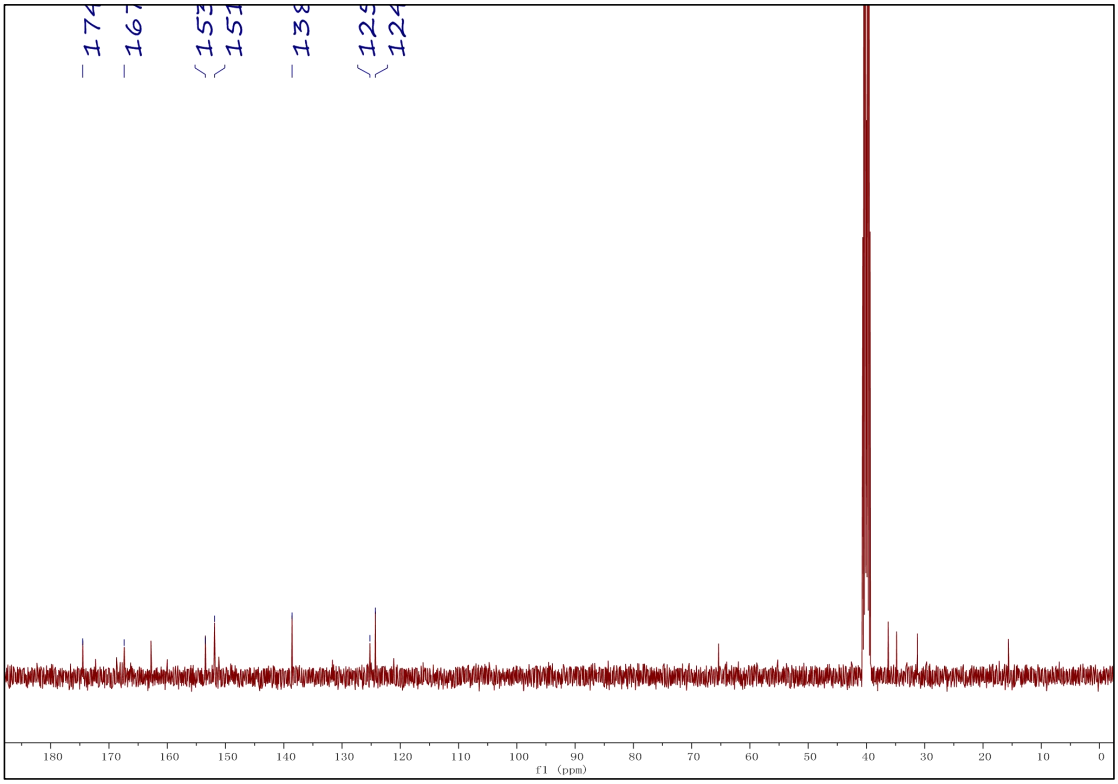

Figure S4. ^{13}C NMR spectrum of **Pt-2** measured in DMSO-d_6.

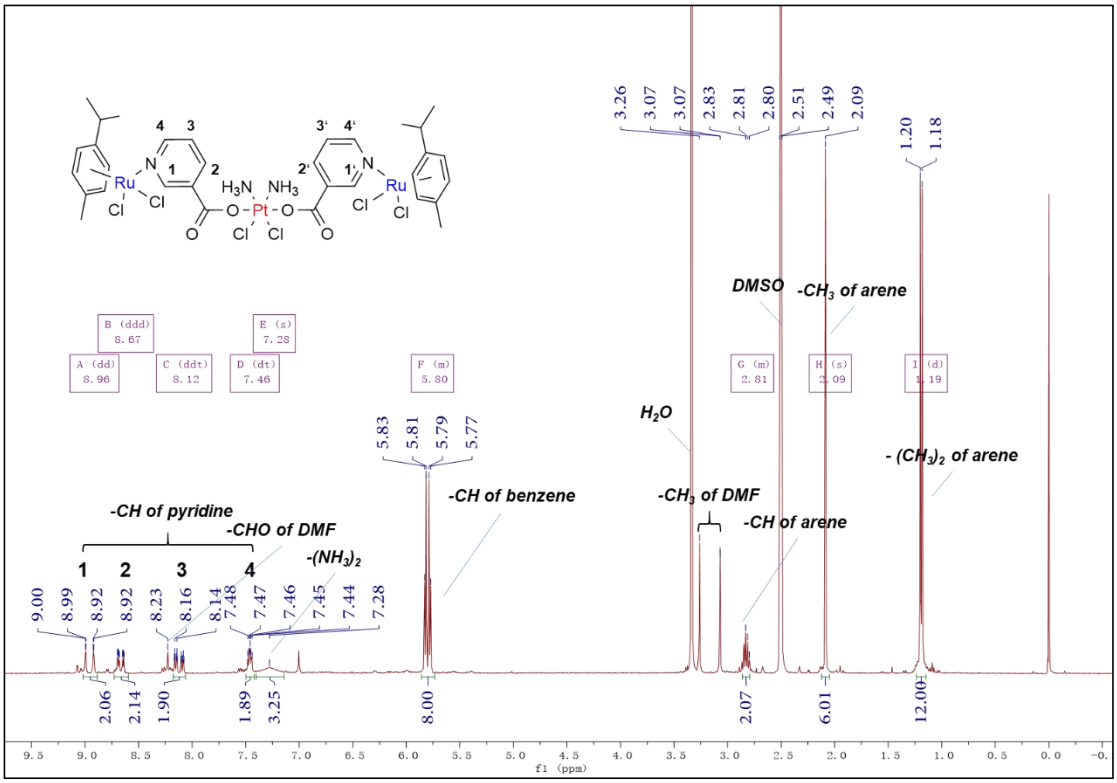

Figure S5. ^{1}H NMR spectrum of **PtRu-1** measured in DMSO-d_6.

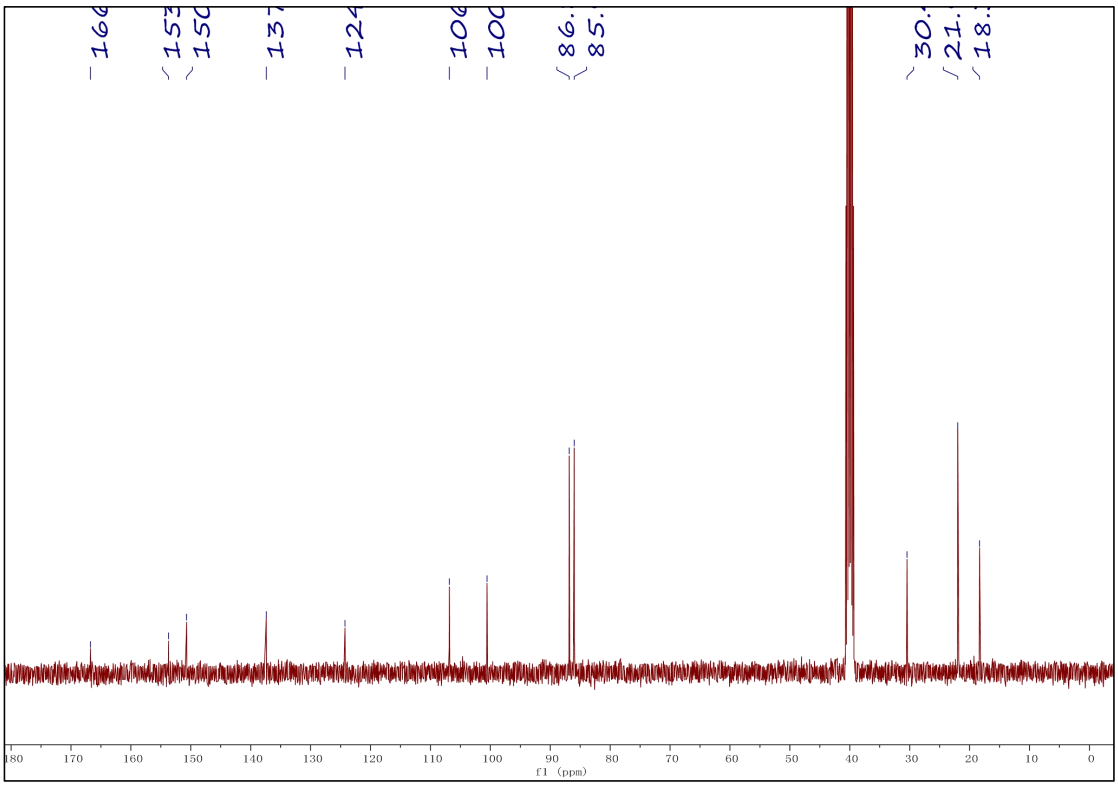

Figure S6. ^{13}C NMR spectrum of **PtRu-1** measured in DMSO-d_6.

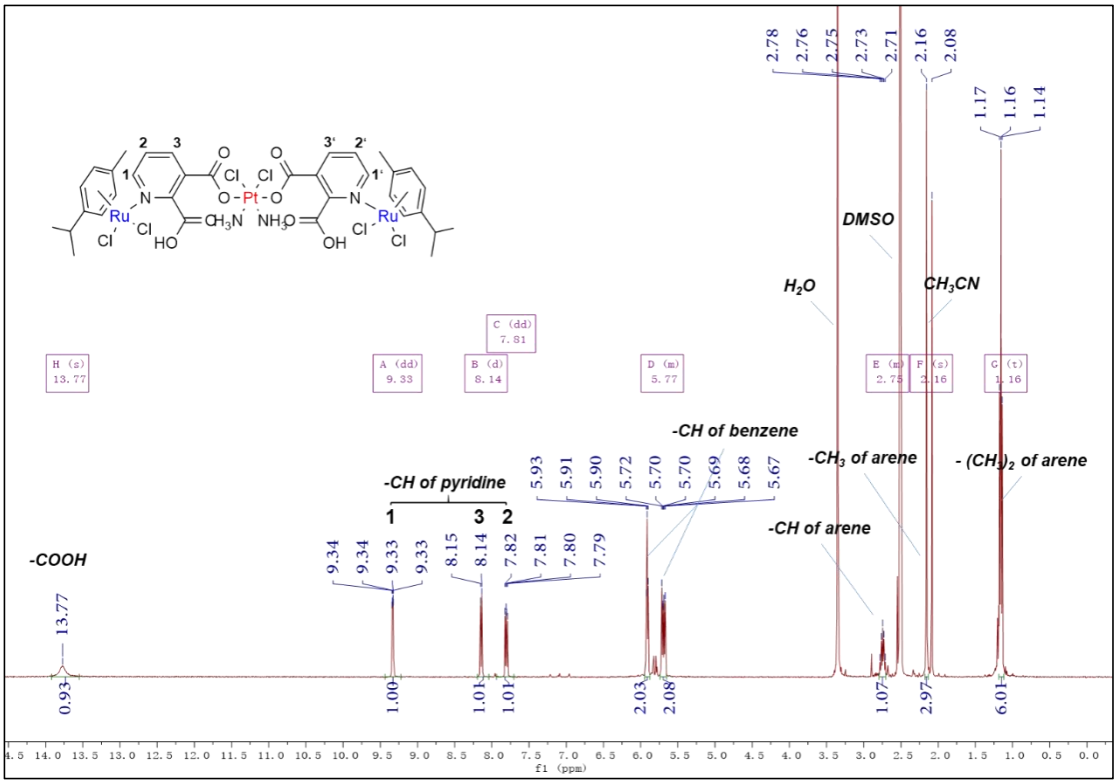

Figure S7. [1]H NMR spectrum of **PtRu-2** measured in DMSO-d_6.

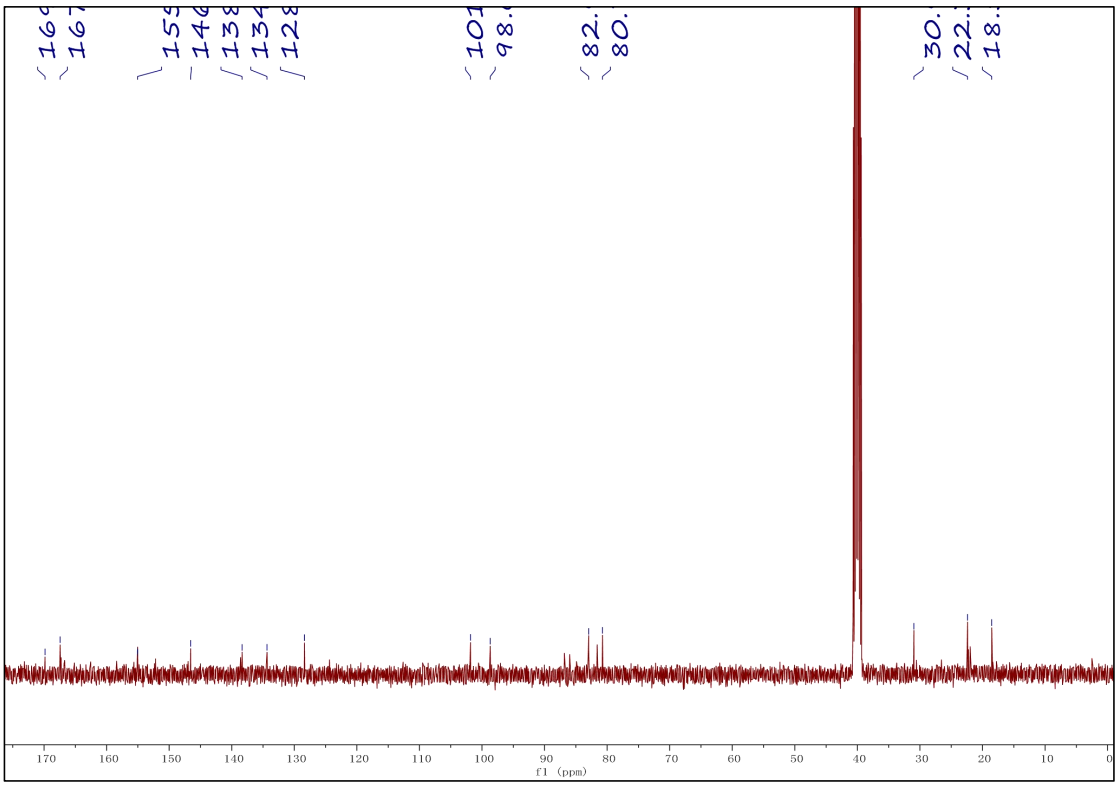

Figure S8. [13]C NMR spectrum of **PtRu-2** measured in DMSO-d_6.

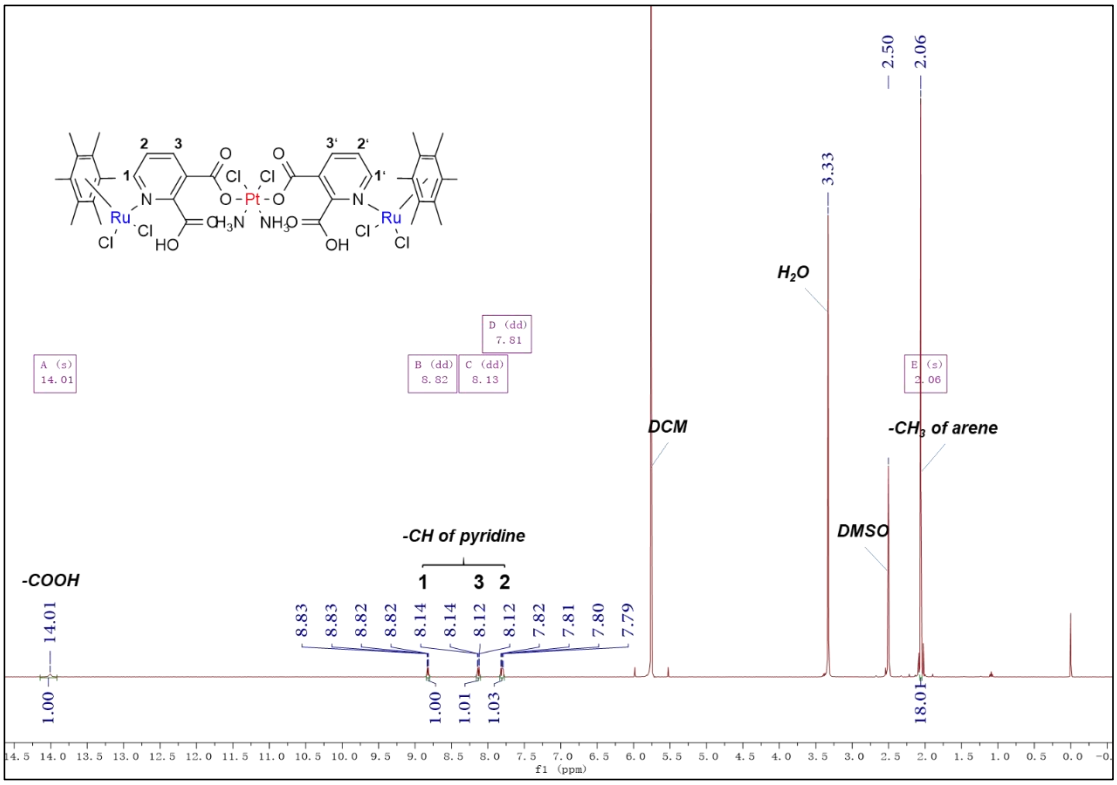

Figure S9. [1]H NMR spectrum of **PtRu-3** measured in DMSO-d_6.

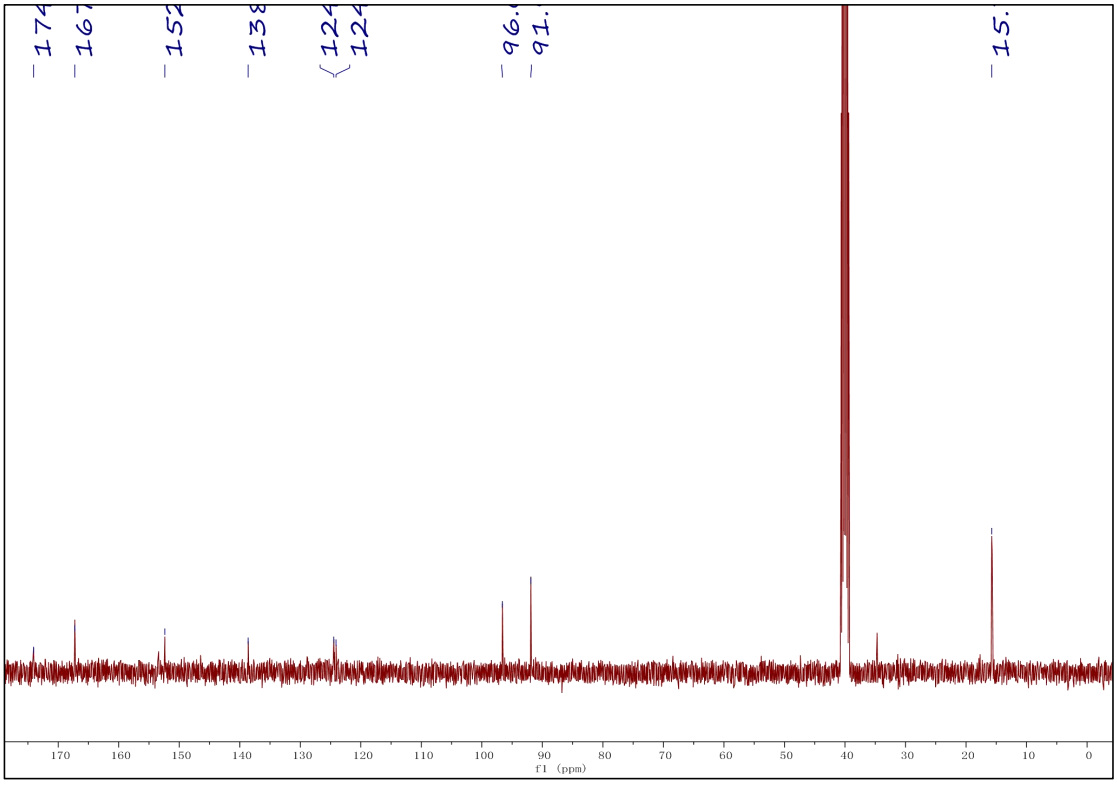

Figure S10. [13]C NMR spectrum of **PtRu-3** measured in DMSO-d_6.

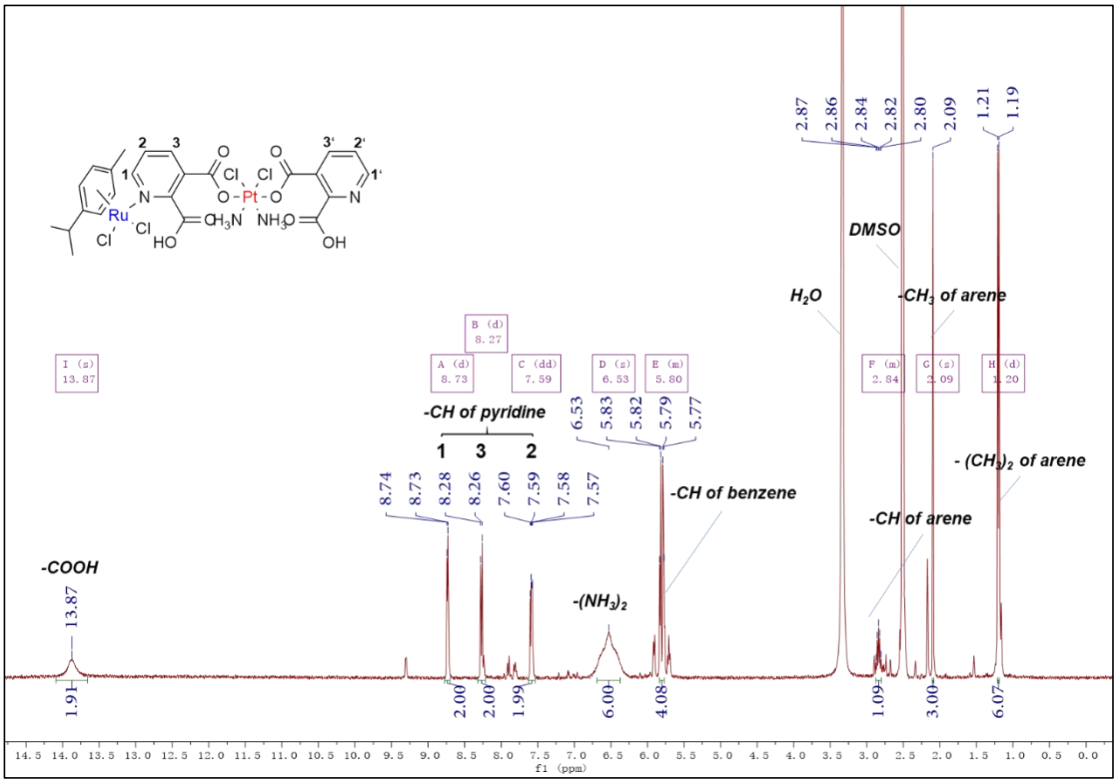

Figure S11. ^{1}H NMR spectrum of **PtRu-4** measured in DMSO-d_6.

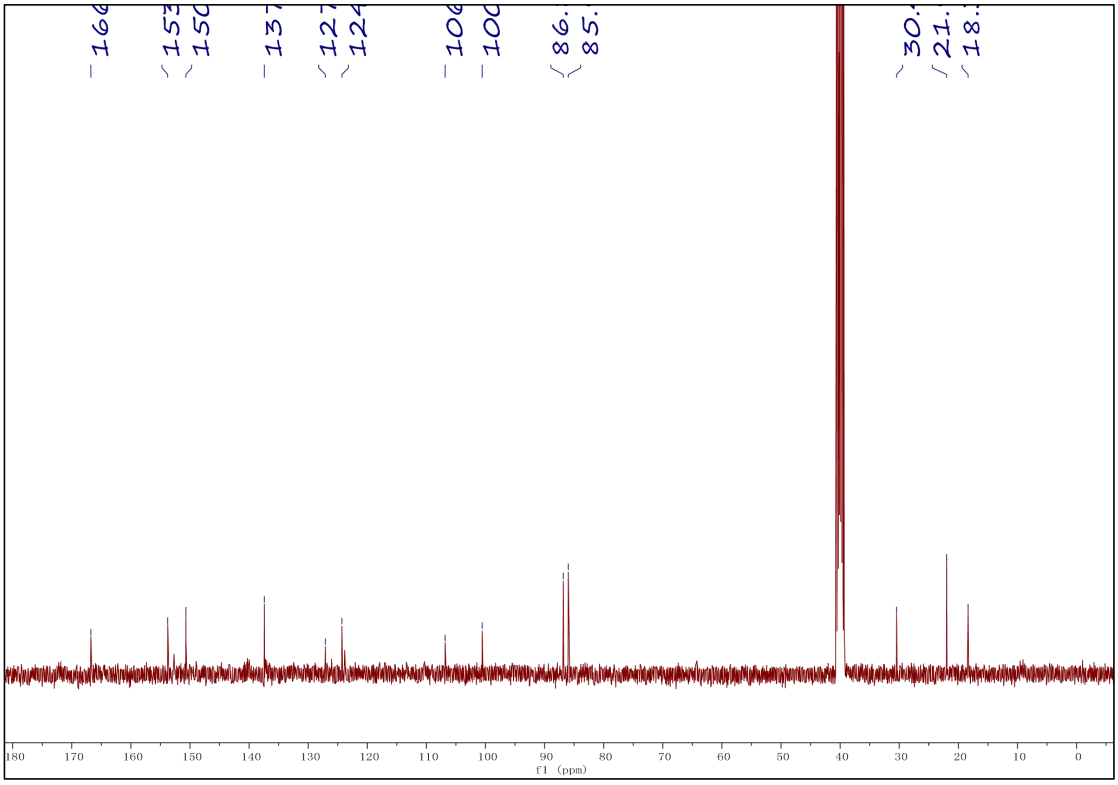

Figure S12. ^{13}C NMR spectrum of **PtRu-4** measured in DMSO-d_6.

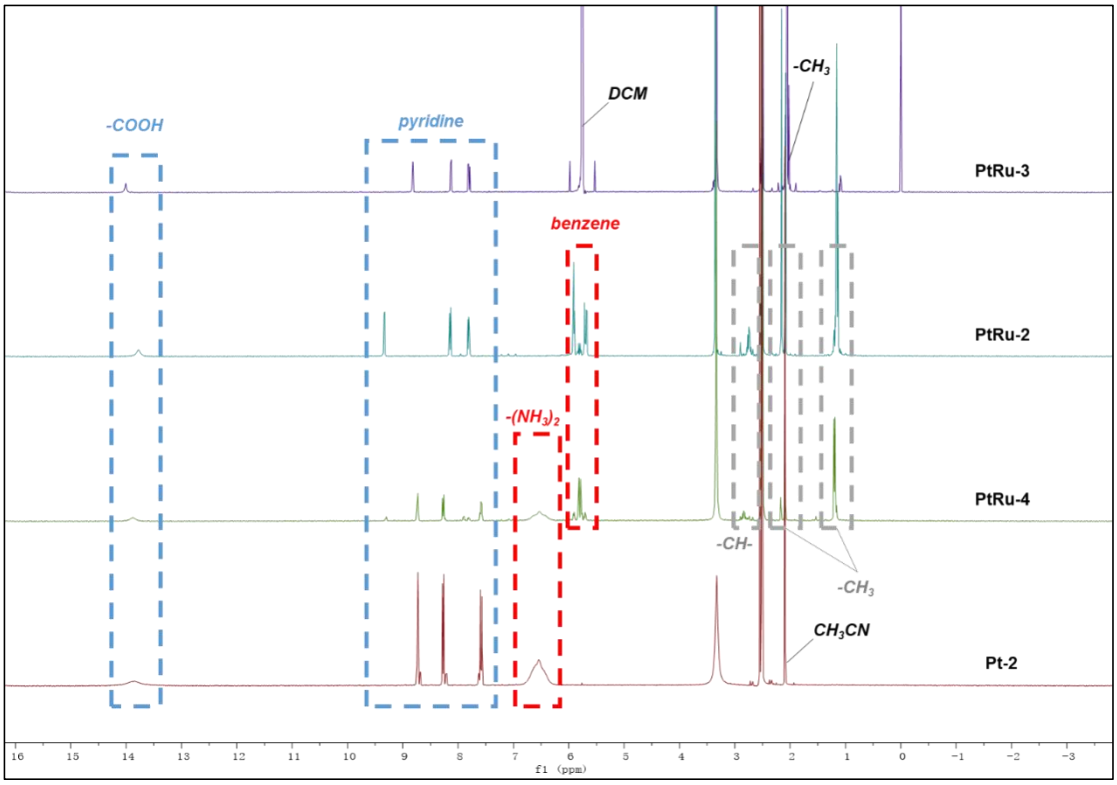

Figure S13. Comparison of ^{1}H NMR spectra for **PtRu-2**, **PtRu-3**, **PtRu-4**, and **Pt-2**.

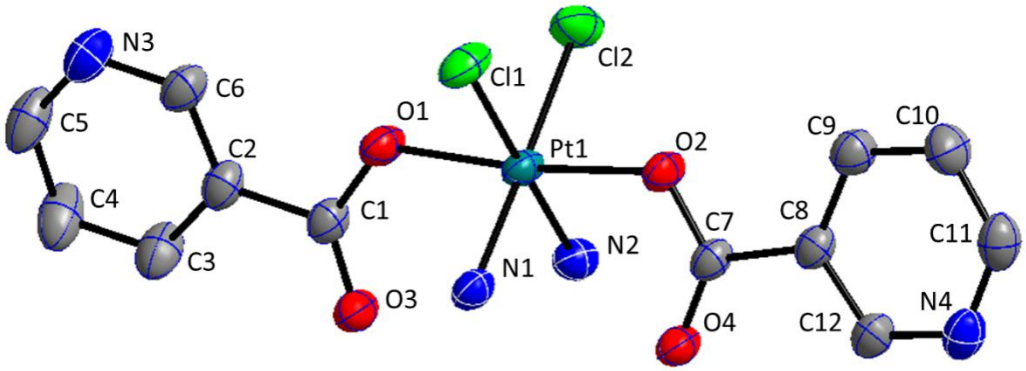

Figure S14. Crystal structure of **Pt-1**.

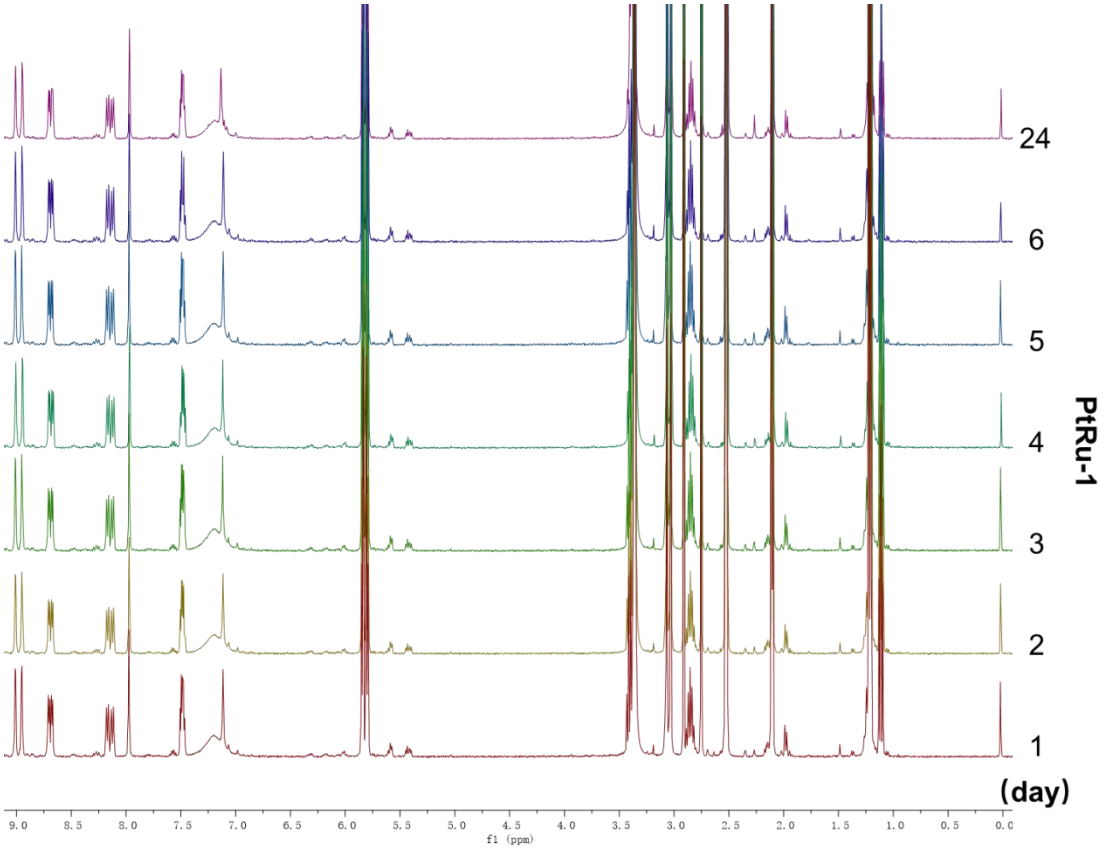

Figure S15. Stability of the complex **PtRu-1** in DMSO as examined by ^{1}H NMR measurements for 24 days. The results showed that no change in the spectra was observed during measurement.

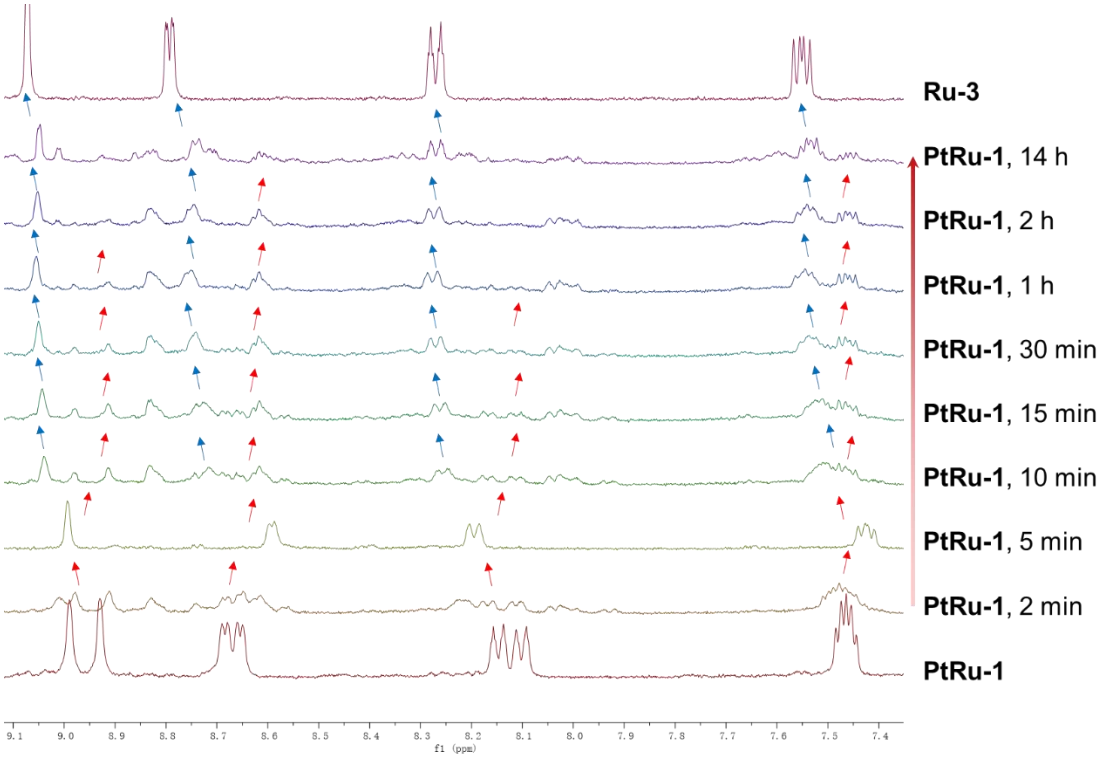

Figure S16. The reduction of **PtRu-1** in the presence of excess sodium ascorbate, as examined by ^{1}H NMR measurements. As time progresses, the characteristic pyridine peaks ascribed to **Ru-3** (blue arrows) appeared, and concurrently, the pyridine peaks ascribed to **PtRu-1** (red arrows) disappeared.

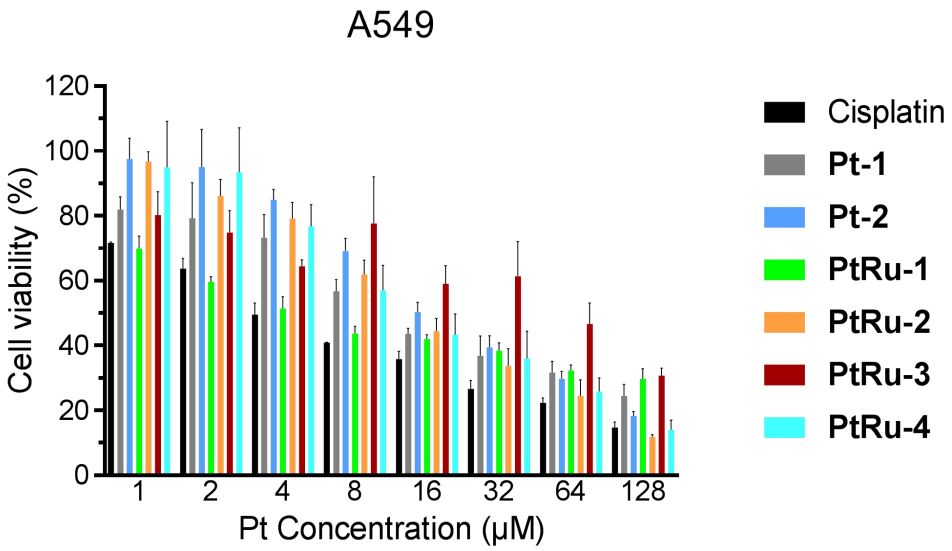

Figure S17. *In vitro* cytotoxicity of the compounds in human lung cancer A549 cells. Cisplatin was included as control. The cells were treated with compounds for 72 h and the viability was determined by the MTT assay.

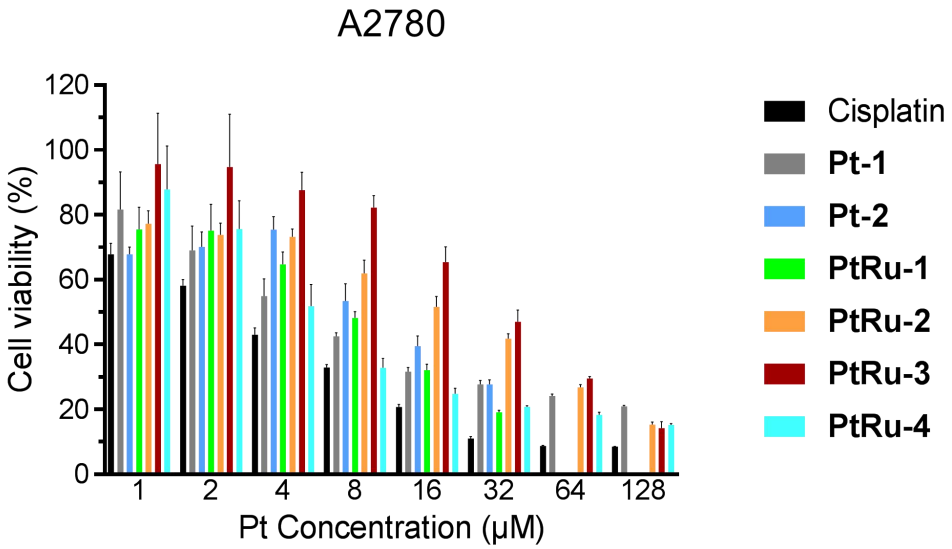

Figure S18. *In vitro* cytotoxicity of cisplatin, platinum-based compounds and bimetal compounds in human ovarian carcinoma A2780 cells.

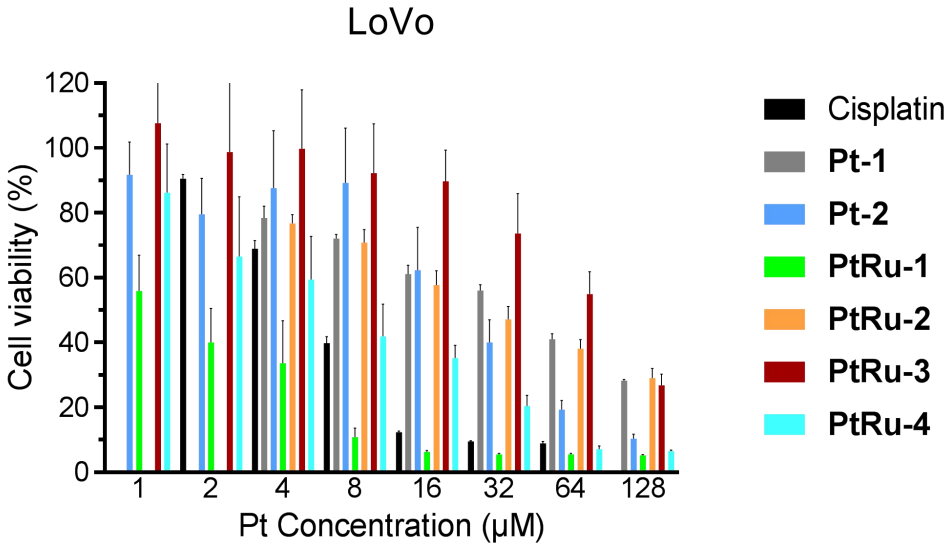

Figure S19. *In vitro* cytotoxicity of cisplatin, Pt-based compounds and bimetal compounds in human colon adenocarcinoma LoVo cells.

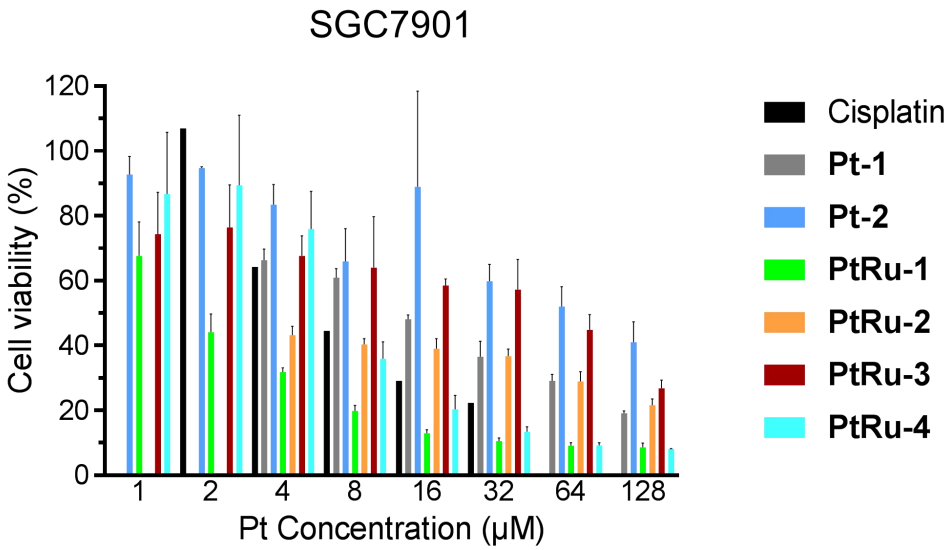

Figure S20. *In vitro* cytotoxicity of cisplatin, Pt-based compounds and bimetal compounds in human gastric cancer SGC7901 cells.

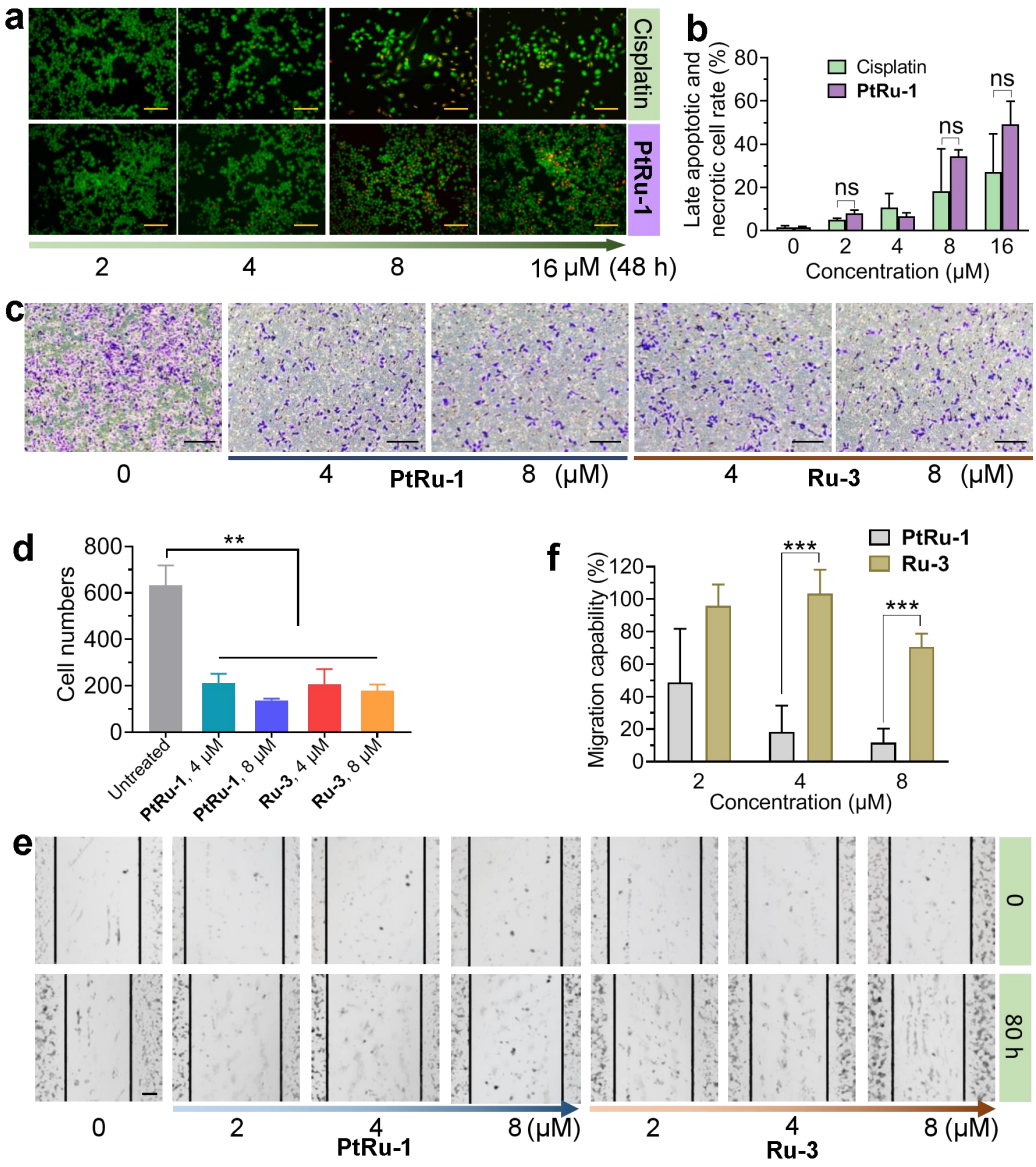

Figure S21. (**a**) *In vitro* cytotoxicity examined by AO/EB double staining assay after the treatment with different concentrations of cisplatin and **PtRu-1**. (**b**) Quantification of the percentage of apoptotic cells. (**c**) Ru complexes **Ru-3** and **PtRu-1** inhibit the invasion of HUVECs. The cells that passed through the Matrigel appear violet when observed under the microscope. (**d**) Quantification of penetrated cells. (**e**) Migration of A2780 cells after the treatment with **PtRu-1** and **Ru-3** for 80 h as determined by a woundhealing assay. Culture medium with 1% FBS. (**f**) Migration capability expressed as the percentage of the distance that cells moved compared with that of untreated cells. ns, not significant, ** $p < 0.01$, *** $p < 0.001$. Scale bars: 200 μm.

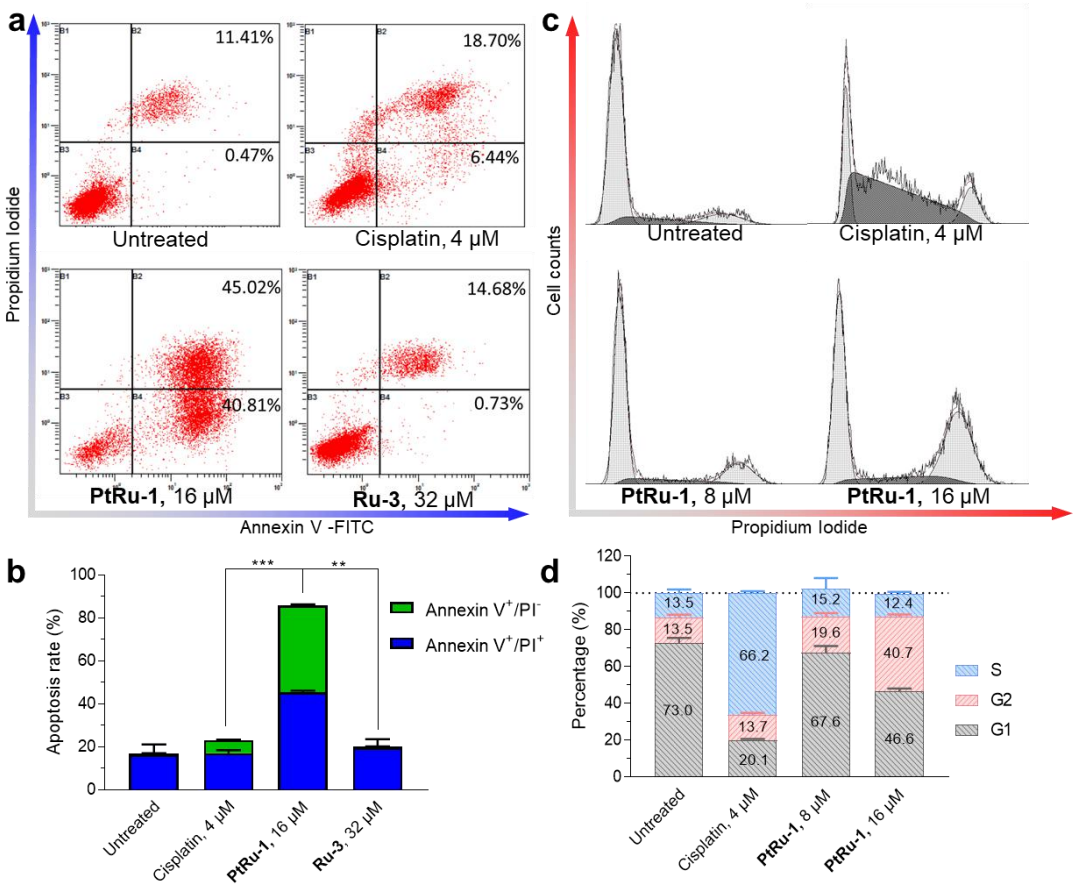

Figure S22. Flow cytometry for analysis of cell cycle and apoptosis. A2780 cells were treated with the compounds for 48 h. (**a**) Apoptosis detected by an FITC Annexin V/PI double staining assay. (**b**) Quantification of the apoptotic cells induced by the compounds. ** $p < 0.01$, *** $p < 0.001$. (**c**) Cell cycle analysis on A2780 cells with different treatments. (**d**) Quantification of the cells arrested at different phases of cell cycle.

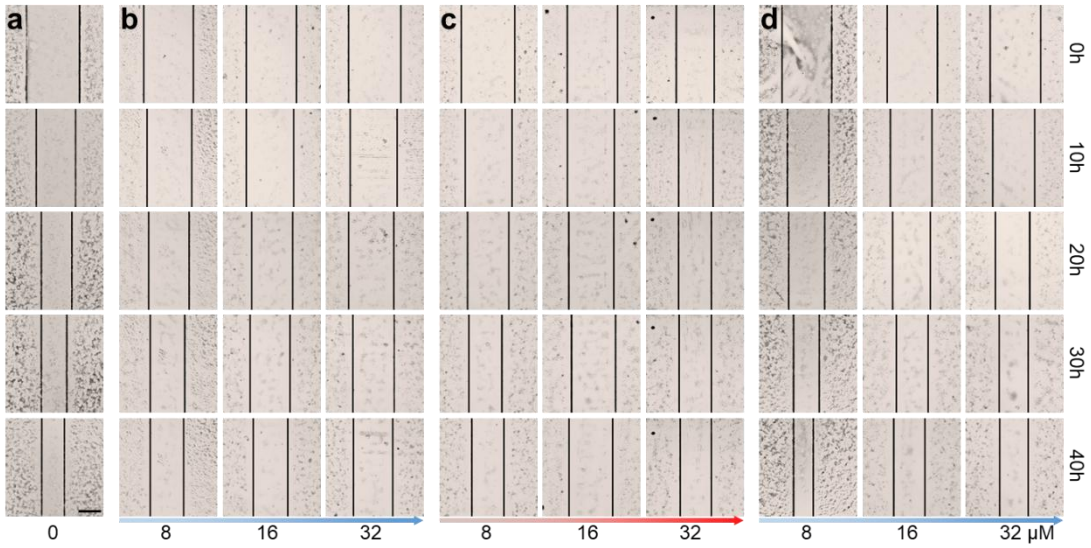

Figure S23. The migration of HUVEC cells was observed by a wound-healing assay. The cells were incubated with (**b**) **Pt-1** (8, 16, and 32 μM), (**c**) **PtRu-1** (8, 16, and 32 μM), and (**d**) **Ru-3** (8, 16, and 32 μM). The cells were photographed by microscopy after predetermined time of incubation. Scale bar: 400 μm.

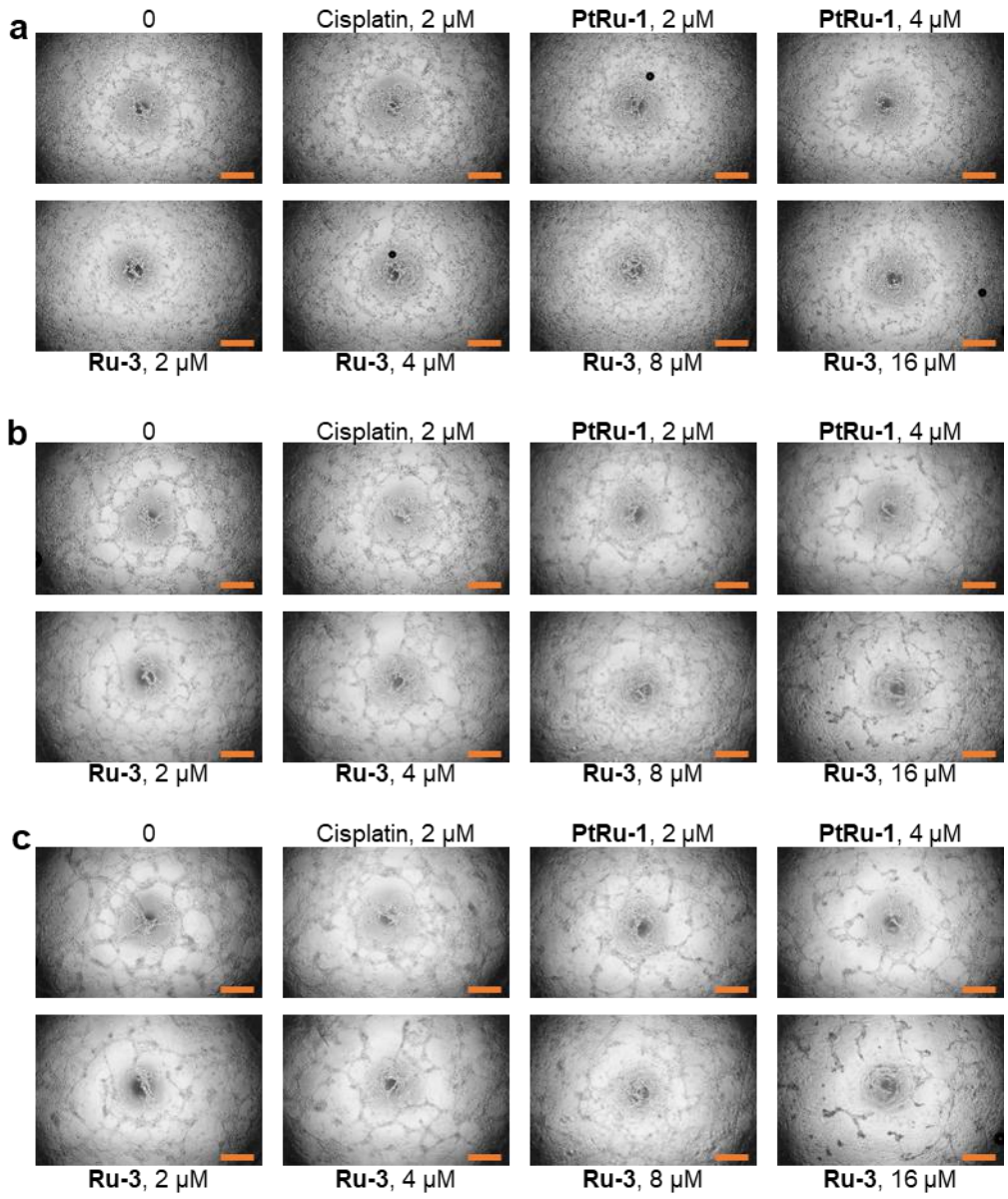

Figure S24. Tube-forming experiment of HUVEC cells after the treatment with the compounds at different concentrations for (**a**) 4 h, (**b**) 8 h, and (**c**) 12 h. Scale bars: 400 μm.

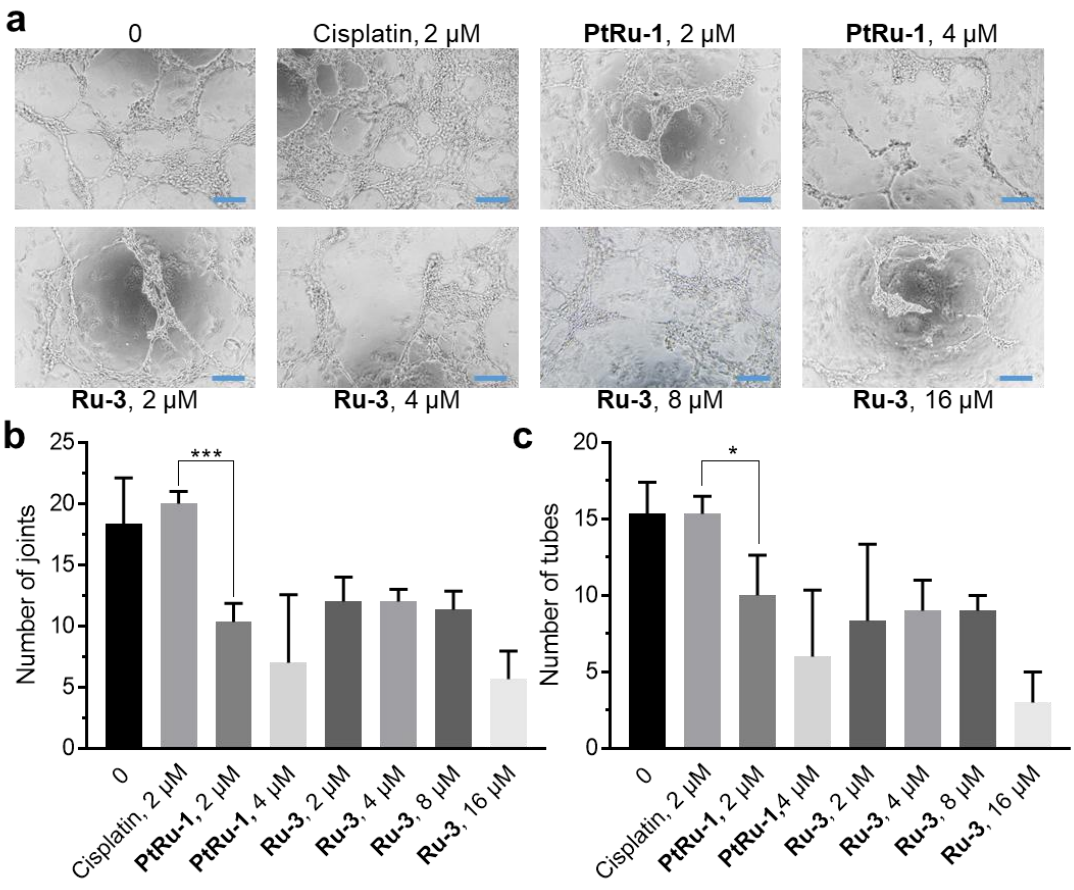

Figure S25. (**a**) Tube-forming experiment of HUVEC cells after the treatment for 12 h. Cisplatin at 2 μM was not effective to inhibit tube formation. Scale bars: 200 μm. (**b**) Number of joints and (**c**) number of formed tubes in different treatment groups.

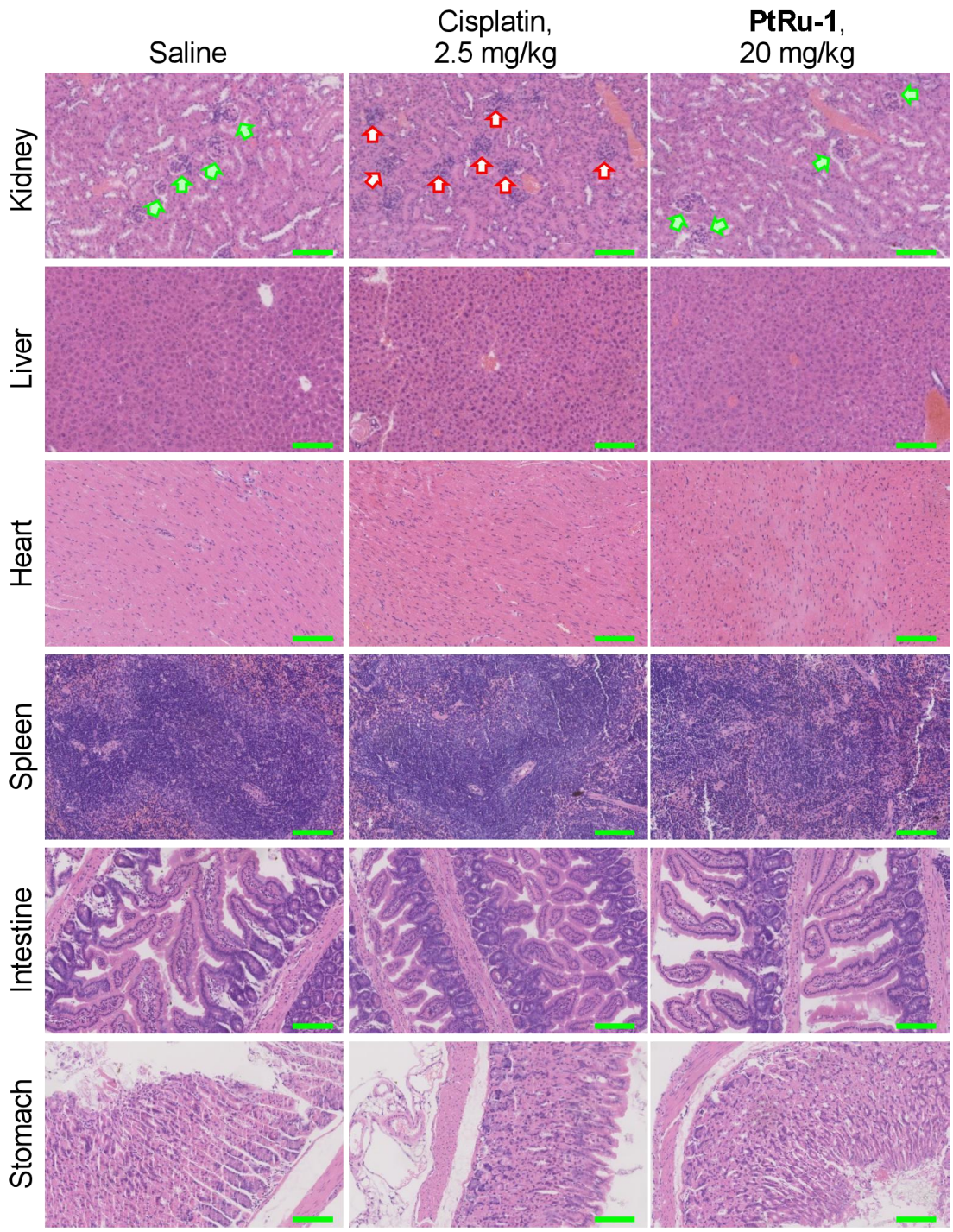

Figure S26. Histopathological examination of the organs excised from the mice after various treatments. Green and red arrows indicate normal and damaged glomeruli in kidney, respectively. No visible damages were observed in heart, spleen, inestine and stomach, indicating low toxicity of **PtRu-1** at a dose of 20 mg/kg (cisplatin equivalent) in animals. Scale bars: 100 μm.

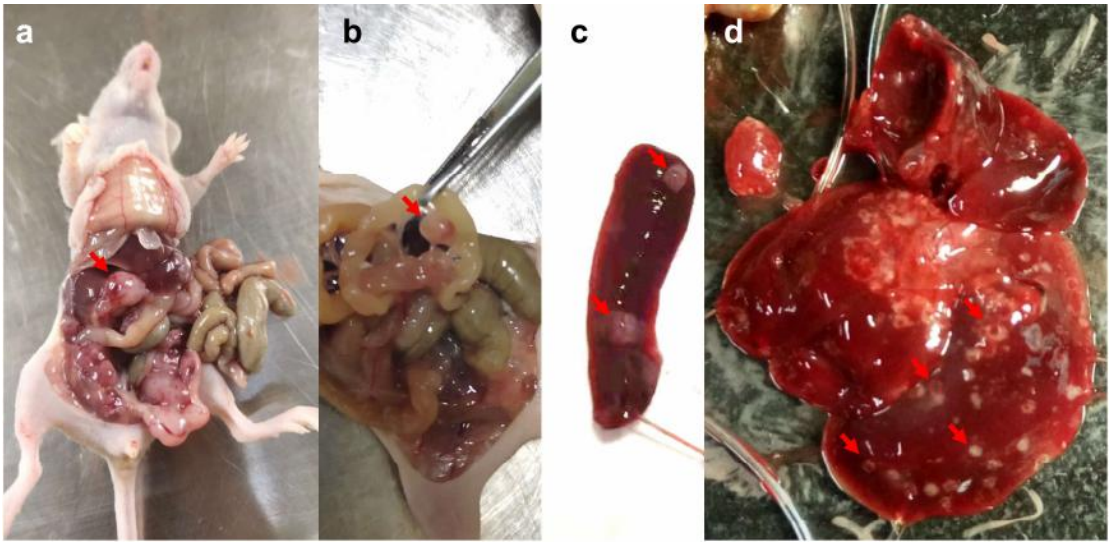

Figure S27. Typical photographs for mouse tumors. Arrows indicate (**a**) abnormal ovary, (**b**) tumors in the abdominal cavity (most of tumors localized within the mesentery), and metastasized tumors in spleen (**c**) and liver (**d**).

Supplementary Tables

Table S1. Crystal data and structure refinement for **Pt-1**.

Compound	**Pt-1**
Formula	$C_{22}H_{38}Cl_2N_6O_7Pt$
$D_{calc.}$/ g cm^{-3}	1.665
m/mm^{-1}	4.825
Formula Weight	764.57
Colour	colourless
Shape	block
Size/mm^3	0.53×0.33×0.20
T/K	170(2)
Crystal System	triclinic
Space Group	P-1
a/Å	12.7146(6)
b/Å	15.4589(7)
c/Å	16.8740(8)
a/°	90.091(2)
b/°	111.105(2)
g/°	99.087(2)
V/Å^3	3049.2(2)
Z	4
Z'	2
Wavelength/Å	0.71073
Radiation type	MoK$_a$
Q_{min}/°	2.33
Q_{max}/°	27.143
Measured Refl.	116227
Independent Refl.	13460
Reflections with I > 2(I)	12271
R_{int}	0.0566
Parameters	731
Restraints	130
Largest Peak	0.977
Deepest Hole	-0.796
GooF	1.047
wR_2 (all data)	0.0528
wR_2	0.051
R_1 (all data)	0.0244
R_1	0.0212

Table S2. Selected bond lengths (Å) and angles (˚) for **Pt-1**.

Bond lengths Å	
Pt1-Cl1	2.3177(7)
Pt1-Cl2	2.3197(7)
Pt1-O2	2.0030(18)
Pt1-O4	2.0028(18)
Pt1-N2	2.042(2)
Pt1-N3	2.044(2)

Angles (˚)	
Cl1-Pt1-Cl2	93.00(3)
O2-Pt1-Cl1	87.71(6)
O2-Pt1-Cl2	88.63(6)
O2-Pt1-N2	91.97(8)
O2-Pt1-N3	91.15(8)
O4-Pt1-Cl1	87.86(6)
O4-Pt1-Cl2	86.26(6)
O4-Pt1-O2	173.06(7)
O4-Pt1-N2	92.38(8)
O4-Pt1-N3	93.91(8)
N2-Pt1-Cl1	179.16(7)
N2-Pt1-Cl2	86.22(7)
N2-Pt1-N3	94.45(9)
N3-Pt1-Cl1	86.34(7)
N3-Pt1-Cl2	179.31(7)

Reference:

1. G. M. Sheldrick, *Acta Crystallogr A*, 2015, **71**, 3-8.
2. G. M. Sheldrick, *Acta Crystallogr C Struct Chem*, 2015, **71**, 3-8.
3. L. T. Ellis, H. M. Er and T. W. Hambley, *Aust. J. Chem.*, 1995, **48**, 793-806.
4. R. Kocz, J. Roestamadji and S. Mobashery, *J Org Chem*, 1994, **59**, 2913-2914.